haematologica
Journal of the Ferrata Storti Foundation

The Znf711-Phf8 complex functions as a transcriptional rheostat essential for neutrophil development

by Shuiyi Tan, Huihui Qian, Haihong Wang, Yi Chen, Hao Yuan, Xiaohui Liu, Yujie Wang, Hugues de Thé, Jun Zhu and Jun Zhou

Received: October 30, 2025.
Accepted: February 6, 2026.

Citation: Shuiyi Tan, Huihui Qian, Haihong Wang, Yi Chen, Hao Yuan, Xiaohui Liu, Yujie Wang, Hugues de Thé, Jun Zhu and Jun Zhou. The Znf711-Phf8 complex functions as a transcriptional rheostat essential for neutrophil development.
Haematologica. 2026 Feb 19. doi: 10.3324/haematol.2025.300134 [Epub ahead of print]

The Znf711-Phf8 complex functions as a transcriptional rheostat essential for neutrophil development

Shuiyi Tan[1,2,3]*, Huihui Qian[1,2]*, Haihong Wang[1,2], Yi Chen[1], Hao Yuan[1,2], Xiaohui Liu[1,2], Yujie Wang[1,2], Hugues de Thé[2,4], Jun Zhu[2,4#], Jun Zhou[1,2#]

1 Shanghai Institute of Hematology, State Key Laboratory of Medical Genomics, National Research Center for Translational Medicine at Shanghai, Ruijin Hospital, Shanghai Jiao Tong University School of Medicine, Shanghai 200025, China

2 CNRS IRP (International research Project), Cancer, Aging and Hematology, Sino-French Research Center for Life Sciences and Genomics, Ruijin Hospital, Shanghai Jiao Tong University School of Medicine, Shanghai 200025, China

3 Department of Hematology, Huashan Hospital, Fudan University, Shanghai 200040, China

4 Université Paris Cité/INSERM/CNRS UMR 1342/8000, Hôpital St. Louis, Paris 75010, France

*These authors contribute equally to this work.

#Correspondence: Dr. Jun Zhou, e-mail: zj10802@rjh.com.cn, Tel: 008621-64453969, ORCID identifier: 0000-0003-0472-3188; Dr. Jun Zhu, e-mail: jun.zhu@paris7.jussieu.fr, Tel: 008621-64453969, ORCID identifier: 0000-0002-7983-3130

Running head: The Znf711-Phf8 complex regulates granulopoiesis

Declaration of Interests

The authors declare no competing interests.

Author Contributions

S. T and H.Q conducted most of the experiments and analyzed data. H.W conducted

FACS analyses and cell sorting. Y.C maintains the zebrafish lines. H.Y, X.L, and Y. W performed RNA-seq, and conducted analysis of the RNA-seq data. H.d.T provided advice regarding the experiments. J.Z provided advice and analyzed data. J.Z designed the project, analyzed data, and wrote the manuscript.

Data availability

RNA sequencing dataset generated in this study is available in the Gene Expression Omnibus (GEO) database (GSE295370).

Acknowledgments

The authors would like to express their gratitude to Prof. Yiyue Zhang (from the School of Medicine, South China University of Technology, Guangzhou, People's Republic of China) for providing the *gfi1aa* knockout line, and Dr. Xinfu Jiao (from the Department of Cell Biology and Neuroscience, Rutgers University, Piscataway, NJ 08854, USA) for his critical manuscript reading. This work was supported by research funding from the National Natural Science Foundation of China (32471154) to Jun Zhou.

Abstract

Neutrophil differentiation is governed by a precise transcriptional and epigenetic program. Here, we identify the zinc finger protein 711 (Znf711) and its partner, the histone demethylase PHD finger protein 8 (Phf8), as essential regulators of terminal granulopoiesis. Contrary to their established role as a transcriptional activator-coactivator pair, we found that the Znf711-Phf8 complex operates through a repressive mechanism. Znf711 promotes neutrophil maturation in a DNA-binding-independent manner by sequestering Phf8. Upon loss of Znf711, Phf8 is recruited by the growth factor independent 1 transcription repressor (Gfi1aa) to the promoter of the master regulator *c/ebpα*, where SUMOylated Phf8 acts as a corepressor to inhibit its transcription. Furthermore, we delineate a positive feedback loop wherein C/ebpα directly activates *znf711* expression, ensuring a high level of *c/ebpα* at the onset of differentiation. Our findings define the Znf711-Phf8 complex as a critical transcriptional rheostat in neutrophil development.

word count: 142 words for the abstract, and 3692 words for the main text.

Introduction

Neutrophils are a vital component of the immune system, acting as the first responders to infections and playing a critical role in combating invading pathogens [1]. As the most abundant type of short-lived white blood cells, they require continuous daily replenishment from hematopoietic stem cells (HSCs). Within the classical hierarchy of hematopoiesis, HSCs sequentially differentiate into common myeloid progenitors (CMPs) and granulocyte-monocyte progenitors (GMPs), which ultimately give rise to the neutrophil and macrophage lineages. This process culminates in terminal differentiation to achieve full neutrophil maturation [2].

The steady-state production of mature neutrophils is tightly regulated by a variety of transcription factors and cofactors [3,4]. Pioneering studies have demonstrated that key transcription factors such as the C/EBP and ETS family proteins act in succession to drive neutrophil development [5]. Concurrently, various epigenetic regulators including histone methyltransferases, histone demethylases (KDMs), and histone deacetylases (HDACs) collaborate with lineage-specific transcription factors throughout the process of neutrophil differentiation [6]. Mutations or abnormal expression of these critical regulators are closely associated with pathologies such as neutropenia or leukemia [7]. Despite extensive research in this area, the full spectrum of regulators involved in neutrophil development and their precise mechanisms remain to be fully elucidated.

The human *ZNF711* gene encodes a C2H2-type transcription factor characterized by a Zfx/Zfy transcription activation region at the N-terminus and thirteen consecutive zinc finger motifs at the C-terminus [8]. Multiple loss-of-function mutations within this gene have been identified in several families with X-linked intellectual disability [9]. Mechanistic studies in neuronal cells have demonstrated that ZNF711 functions as a transcriptional activator by recruiting the histone demethylase PHF8 to activate *KDM5C* expression in neuronal cells [10,11]. Thus, a tight functional link between ZNF711 and PHF8 has been established in the context of neurodevelopmental disorders [10,11].

In addition to its expression in the brain, *ZNF711* is also widely expressed in myeloid lineages [12]. Notably, *ZNF711* is highly expressed at the early stages

(myeloblast and promyelocyte) of terminal granulopoiesis but significantly declines as neutrophils undergo differentiation (the BloodSpot database) (Fig S1A). Consistent with a potential role in leukemogenesis, lowered expression of *ZNF711* has been observed in most acute myeloid leukemia (AML) subtypes (the BloodSpot database) (Fig S1A). Additionally, the BeatAML database [13] includes five cases harboring *ZNF711* mutations: four carry missense mutations of unknown significance, and one carries a truncating mutation ($ZNF711^{E316/*}$), which deletes part of the transcription activation region, the nuclear localization signal (NLS), and all zinc finger motifs, rendering it a loss-of-function mutation (Fig S1B). The expression profile, coupled with the AML-associated mutation, strongly suggests potential roles for *ZNF711* in both normal myelopoiesis and its malignant counterpart. However, its precise function in hematopoiesis remains to be elucidated.

PHF8 contains a PHD finger that mediates binding to specific nuclear protein partners and chromatin, as well as a Jumonji C (JmjC) domain exhibiting histone demethylase catalytic activity [14,15]. Thus, PHF8 is generally identified as a transcriptional coactivator that removes repressive histone marks to activate gene expression [14–16]. Notably, amplification of *PHF8* has been frequently observed in AML patients (The Cancer Genome Atlas database). Furthermore, PHF8 is a proven regulator of the cell-intrinsic immune response in AML, as its transduction impedes leukemic transformation and suppresses clonogenic growth while facilitating apoptosis of AML cells [17]. Conversely, in chronic myeloid leukemia (CML), PHF8 inhibits differentiation of CML cells and promotes their proliferation by activating transcription of the *BCR-ABL1* fusion gene [18]. These contradictory findings suggest that the role of PHF8 in leukemogenesis is context-dependent and intricate. Similar to *ZNF711*, the potential functions of *PHF8* in normal myelopoiesis also remain unclear.

In this study, we generated two knockout zebrafish lines to demonstrate that both *znf711* and *phf8* are essential for neutrophil development. Mechanistically, we found that Znf711 and Phf8 do not function synergistically as a canonical combination of transcriptional activator and coactivator during this process. Instead, Znf711 acts in a DNA-binding-independent manner by impeding its partner Phf8 from inhibiting the

expression of *c/ebpα*, the master regulator driving granulopoiesis. Concurrently, rather than functioning solely as a canonical histone demethylase that activates transcription, Phf8 serves as an important corepressor of the transcription factor Gfi1aa to regulate neutrophil maturation. Moreover, we demonstrate that SUMOylation is required for Phf8 to engage in transcriptional repression. Finally, we identified a positive feedback loop between *c/ebpα* and *znf711*, which ensures a high level of *c/ebpα* expression at the early stages of terminal granulopoiesis to promote cell differentiation. Overall, our findings reveal that Znf711 and Phf8 are two novel and critical regulators in terminal granulopoiesis that operate through a fine-tuned transcriptional regulatory circuit centered on *c/ebpα*.

Methods

Zebrafish strains

Zebrafish strains including Tubingen, Tg(*mpx*:GFP), *znf711*, *phf8*, and *gfi1aa* homozygous mutants, were raised under standard conditions (28.5°C in system water). All animal work was approved by the Ethics Committee of Ruijin Hospital Affiliated to Shanghai Jiao Tong University School of Medicine.

Procedures and methods

Detailed information about generation of *znf711* and *phf8* knockout lines using CRISPR/Cas9 system, morpholinos, whole-mount *in situ* hybridization (WISH), Sudan Black staining, FACS analysis and cell collection, RNA-seq and RT-qPCR, plasmid construction, dual-luciferase reporter assay, co-immunoprecipitation (co-IP) and western blot assay, chromatin immunoprecipitation qPCR (ChIP-qPCR), cell lines and treatment are provided in the “Supplemental Methods”.

Statistical analysis

Data were analyzed by GraphPad Prism 9.0 software using two tailed Student's *t*-test for comparisons between two groups and one-way analysis of variance (ANOVA) among multiple groups. Differences were considered significant at $P < 0.05$. Data are expressed as mean ± standard error of the mean (SEM).

Data availability

RNA sequencing dataset generated in this study is available in the Gene Expression Omnibus (GEO) database (GSE295370).

Results

Zebrafish *znf711* is required for neutrophil development across the lifespan

The zebrafish (Danio rerio) has emerged as a powerful model for hematopoietic research over the past two decades [19]. Given the high evolutionary conservation between zebrafish Znf711 and its human ortholog (Fig S2), we sought to define its role in hematopoiesis. We generated a *znf711* knockout zebrafish line using the CRISPR/Cas9, resulting in a truncated protein that lacked the Zfx/Zfy transactivation domain, the nuclear localization signal (NLS), and all zinc finger motifs (Fig S3A, B). RT-qPCR data confirmed the significant reduction of *znf711* transcripts in the homozygous mutants (Fig S3C).

Zebrafish hematopoiesis occurs in two waves, primitive and definitive, at distinct anatomical sites [20,21]. Primitive neutrophils and monocytes/macrophages originate from the rostral blood island (RBI), while the intermediate cell mass (ICM) gives rise to primitive erythrocytes and some neutrophils [22,23]. During definitive hematopoiesis, HSCs emerge from the ventral wall of the dorsal aorta (VDA), migrate to the caudal hematopoietic tissue (CHT), and finally colonize the kidney marrow (KM) in adults [22,23].

To dissect the function of *znf711* in hematopoiesis, we performed whole-mount *in situ* hybridization (WISH) with lineage-specific markers on mutant embryos and larvae. At 22 hours post-fertilization (hpf), the development of primitive monocytes/macrophages and erythrocytes was unperturbed in *znf711* mutants (Fig S4). In sharp contrast, expression of neutrophil markers including *c/ebp1* (the zebrafish ortholog of human *C/EBPε*), *lysozyme* (*lyz*), and *myeloperoxidase* (*mpx*), was significantly impaired in primitive neutrophils derived from both the RBI and ICM (Fig 1A-D', N).

This neutrophil-specific defect persisted into the definitive hematopoiesis stage, with no apparent impact on other lineages (Fig S4). From 36 hpf to 5 days post-fertilization (dpf), we observed a marked reduction in the expression of *c/ebp1*, *lyz*, and *mpx* (Fig 1E-K', N). The impairment in neutrophil development was further confirmed by Sudan Black (SB) staining (Fig 1L, L', N) and by a pronounced reduction of GFP^+ cells in *znf711*$^{-/-}$//*Tg(mpx:eGFP)* larvae at 48 hpf (Fig 1M, M', N).

The specificity of this phenotype was confirmed by the following experiments: knockdown of *znf711* with specific morpholino antisense oligonucleotides (MO) in wild-type embryos recapitulated the neutrophil deficiency, and this defect was fully rescued by reintroducing either zebrafish *znf711* or human *ZNF711* mRNA (Fig 1O, P). The functional complementation by human *ZNF711* indicates that its role in granulopoiesis is evolutionarily conserved.

To determine whether this requirement extends into adulthood, we analyzed whole kidney marrow (WKM) from one-year-old zebrafish. Fluorescence-activated cell sorting (FACS) revealed a significant decrease in both the percentage of GFP^+ cells within the myeloid gate (87.4% vs. 39.0%) and the GFP fluorescence intensity in *znf711*$^{-/-}$//Tg(*mpx:eGFP*) mutants compared to controls (Fig 2A, B). Consistently, May-Grünwald Giemsa staining showed a substantial reduction in the proportion of mature neutrophils (27.4% vs. 8.8%) in the mutants (Fig 2C, D). In contrast, the percentages of cells in the erythrocyte and lymphocyte gates were comparable between WT and mutant WKMs (Fig S5).

In conclusion, our findings demonstrate that Znf711 is a neutrophil-specific

regulator whose function is required throughout the lifespan of zebrafish.

c/ebpα downregulation mediates the neutrophil developmental defect in *znf711* mutants

To gain insight into the mechanism underlying the neutrophil defect in *znf711* mutants, we performed RNA sequencing (RNA-seq) on GFP^+ cells from wild-type Tg(*mpx*:eGFP) and *znf711*$^{-/-}$//Tg(*mpx*:eGFP) larvae at 48 hpf (Supplementary information). A heatmap of differentially expressed genes (DEGs) clearly illustrates the transcriptional alterations in *znf711*-deficient neutrophils (Fig 3A). We found a significant decrease in the expression of *c/ebpα*, a master transcription factor governing neutrophil differentiation [24,25], in the mutant cells. Accordingly, the expression of key C/EBPα target genes [26,27], including *c/ebp1*, *csf3r* (the zebrafish ortholog of human granulocyte colony-stimulating factor receptor, *GCSFR*), as well as the neutrophil-specific markers *mpx* and *lyz*, was markedly reduced. RT-qPCR analysis independently confirmed these findings (Fig 3B).

We hypothesized that the downregulation of *c/ebpα* is the major cause of neutrophil impairment in *znf711* mutants. To test this, we performed a genetic rescue experiment by expressing *c/ebpα* specifically in the neutrophil lineage. To avoid potential confounding effects from misexpression in earlier progenitors, we injected a TOL2(*mpx*:*c/ebpα*) plasmid into *znf711*-deficient embryos. Neutrophil-specific restoration of *c/ebpα* substantially rescued the neutrophil defects (Fig 3C, D). Conversely, overexpression of *znf711* in wild-type embryos led to a significant expansion of the *mpx*$^+$ population, which should be caused by *c/ebpα* upregulation (Fig 3C, D, E). Critically, this expansion was abolished when *znf711* mRNA was co-injected with a TOL2(*mpx*:*c/ebpα*-bZIP) plasmid, which expresses a dominant-negative C/ebpα mutant lacking transactivation capacity [28] (Fig 3C, D).

Altogether, these results demonstrate that the deficiency of *znf711* impairs neutrophil development by reducing *c/ebpα* expression.

Znf711 antagonizes Phf8-mediated repression of *c/ebpα* to promote neutrophil

development

To delineate how Znf711 regulates neutrophil differentiation, we began by mapping its functional domains. Strikingly, *in vivo* rescue assays revealed that the mutant lacking the entire DNA-binding domain (Znf711 ΔDBD) restored neutrophil development as effectively as the wild-type protein. By contrast, the mutant lacking the Zfx/Zfy domain (Znf711 ΔZfx/Zfy) was completely non-functional (Fig 4A, B). These results indicate that Znf711 functions in a DNA-binding-independent manner, challenging its canonical role as a transcription factor.

The involvement of the Zfx/Zfy domain in mediating interactions between Znf711 and its partners [29] led us to hypothesize that the loss of Znf711 may release certain interactant, which subsequently inhibits *c/ebpα* expression. We focused on PHF8, a known ZNF711-interacting partner in neurons that typically functions as a transcriptional coactivator [16,30]. Intriguingly, intergrated ChIP-seq and RNA-seq data from wild-type and *PHF8*-depleted HeLa cells suggest that PHF8 can also repress transcription [31], coupled with the finding that PHF8 binds the *C/EBPα* promoter in human myeloid cells (the Cistrome database) [32] (Fig S6). We therefore proposed a model wherein the absence of Znf711 releases Phf8, which in turn represses *c/ebpα* to block neutrophil maturation.

To validate this hypothesis, we first examined whether Phf8 interacts with Znf711 in myeloid cells. Co-immunoprecipitation (co-IP) assays in 32Dcl3 cells (a murine myeloid progenitor cell line) confirmed this interaction using endogenous antibodies (Fig 4C). Further co-IP assays in HEK293T cells demonstrated that the interaction with Phf8 is mediated by the Zfx/Zfy domain of Znf711 (Fig 4D).

Second, we evaluated whether Phf8 inhibits the *c/ebpα* promoter using dual-luciferase reporter assays. Overexpression of *phf8* significantly repressed the promoter, while depletion of endogenous *PHF8* using shRNA activated it (Fig 4E, lanes 1-3). The role of PHF8 as a histone demethylase depends on its H3K4me3-binding PHD finger motif and catalytic JmjC domain [14–16]. Notably, the ΔPhd finger and ΔJmjC mutants of Phf8 repressed the promoter similarly to wild-type Phf8, indicating that Phf8 does not function as a canonical histone demethylase here (Fig 4E, lanes 4 and 5). Moreover, the

Znf711 ΔDBD mutant activated the promoter comparably to wild-type Znf711 (Fig 4E, lanes 6 and 7), implying this activation is indirect. Indeed, Phf8's repression was markedly impaired in the presence of either wild-type or Znf711 ΔDBD mutant (Fig 4E, lanes 8 and 9).

Third, we investigated Phf8 binding to the *c/ebpα* promoter using *in vivo* ChIP-qPCR. Due to the technical challenge of performing chromatin immunoprecipitation on the limited number of GFP^+ cells that can be practically isolated from zebrafish larvae, we conducted these assays in whole larvae expressing HA-Phf8. Even within this heterogeneous cellular context, we observed specific enrichment of the endogenous *c/ebpα* promoter. This enrichment was significantly greater in *znf711*$^{-/-}$ zebrafish (Fig 4F). This result provides direct *in vivo* evidence that Znf711 loss leads to increased occupancy of Phf8 on the *c/ebpα* promoter, consistent with our model that Znf711 sequesters Phf8 from chromatin.

Finally, knockdown of *phf8* in *znf711*-deficient embryos restored *mpx*$^+$ cells to normal levels (Fig 5A, B). Additionally, we also generated a *phf8* knockout line (Fig S7), which exhibited expanded *mpx*$^+$ cells (Fig 5C, D) and a profound (~18-fold) increase in *c/ebpα* expression within these cells (Fig S8A). Notably, *znf711* MO failed to reduce neutrophils in *phf8*$^{-/-}$ zebrafish (Fig 5C, D), indicating that *znf711* is epistatic to *phf8*.

In summary, our findings indicate that neither Znf711 nor Phf8 functions as a canonical transcriptional activator or coactivator. Instead, Znf711 promotes neutrophil development by sequestering Phf8, thereby preventing Phf8-mediated repression of *c/ebpα*.

Gfi1aa recruits Phf8 to the *c/ebpα* promoter to exert transcriptional repression

Previous studies indicate that PHF8 is recruited to the promoters of target genes through interactions with specific transcription factors [33]. Given the DNA-binding-independent role of Znf711 in neutrophil development, we investigated how Phf8 is recruited to the *c/ebpα* promoter.

We focused on Gfi1aa (the zebrafish ortholog of GFI1) for three reasons: i) it is a well-characterized transcriptional repressor expressed in early neutrophils [34]; ii) it directly cooperates with Lsd1 to repress *c/ebpα* expression in zebrafish neutrophils [35]; and iii) similar neutrophil expansion occurs in *gfi1aa, lsd1* [35], and *phf8*-deficient zebrafish, respectively. We therefore hypothesized that Gfi1aa recruits Phf8 to the *c/ebpα* promoter to exert repression.

To test this, we first confirmed the Gfi1aa-Phf8 interaction by co-IP experiments in both HEK293T (Fig 6A) and 32Dcl3 myeloid cells (Fig 6B). Next, dual-luciferase assays in HEK293T cells showed that overexpression of *gfi1aa* or *phf8* repressed the *c/ebpα* promoter, while their depletion activated it (Fig 6C, lanes 1-6). Critically, the repressive function of each was abolished upon depletion of the other (Fig 6C, lanes 7-8), demonstrating their mutual dependence.

This Gfi1aa-Phf8 axis was further solidified *in vivo*. ChIP-qPCR analyses revealed that Gfi1aa and Phf8 co-occupy the *c/ebpα* promoter (Fig 6D). Importantly, Phf8 binding was drastically reduced in *gfi1aa* mutants (Fig 6D, Fig S8B), indicating that Gfi1aa is essential for recruiting Phf8 to chromatin.

Furthermore, genetic epistasis studies revealed that knockdown of either *phf8* or *gfi1aa* in *znf711* mutants restored neutrophil levels (Fig 5A, B; Fig 6E, F). Conversely, *znf711* knockdown failed to reduce neutrophils in *phf8* or *gfi1aa* mutants (Fig 5C, D; Fig 6E, F), placing *znf711* upstream of both.

Overall, these results establish that Gfi1aa recruits Phf8 to the *c/ebpα* promoter, where it serves as a corepressor to exert transcriptional repression.

SUMOylation enables Phf8 to function as a transcriptional corepressor

Having established that Phf8 functions as a Gfi1aa-dependent corepressor, we sought to define the mechanism underlying its repressive activity. In myeloid cells, GFI1 is known to recruit the LSD1-CoREST repressor complex [36]. We found that PHF8

is dispensable for the integrity of these complexes, as its loss did not affect GFI1-LSD1 or GFI1-RCOR1 interactions (Fig S9), suggesting Phf8 functions through a distinct mechanism.

We therefore considered alternative pathways. SUMOylation is a key post-translational modification that is tightly associated with transcriptional silencing through interactions with corepressor machinery [37,38]. Intriguingly, we detected a ~10 kD adduct on PHF8, consistent with mono-SUMOylation. This finding, coupled with PHF8's repressive role, prompted us to investigate whether SUMOylation imparts repressive activity to PHF8.

We confirmed that PHF8 undergoes SUMOylation in cells (Fig 7A). By mutating candidate lysine residues within SUMO consensus motifs (ΨKXE), we identified K840 as the essential site, as its mutation (K840R) abolished SUMOylation (Fig 7A). The SUMOylation-deficient mutant ($PHF8^{K840R}$) completely failed to repress the *c/ebpα* promoter in dual-luciferase assays (Fig 7B). Crucially, repressive activity was fully restored by fusing this mutant directly to SUMO1 ($PHF8^{K840R}$-SUMO1), underscoring the importance of SUMOylation for Phf8's repressive function (Fig 7B).

These results were further confirmed *in vivo*. Neutrophil-specific expression of the $PHF8^{K840R}$ mutant failed to rescue the expanded mpx^{+} population in *phf8*-deficient zebrafish, whereas the $PHF8^{K840R}$-SUMO1 fusion rescued the phenotype as effectively as wild-type PHF8 (Fig 7C, D).

Taken together, these findings demonstrate that instead of functioning as a canonical transcriptional coactivator, Phf8 serves as a corepressor that collaborates with Gfi1aa to repress *c/ebpα* expression in a SUMOylation-dependent manner.

znf711 is a direct downstream target of C/ebpα

Our previous data placed Znf711 upstream of *c/ebpα* by preventing its repression. To fully delineate this regulatory hierarchy, we examined their expression dynamics

during terminal granulopoiesis. Both *C/EBPα* and *ZNF711* peak at the myeloblast/promyelocyte stages and rapidly decline upon differentiation [34] (the BloodSpot database) (Fig 8A), suggesting potential co-regulation. Since Znf711 safeguards *c/ebpα* expression, we hypothesized that C/ebpα might, in turn, directly activate *znf711*, forming a reinforcing circuit.

Analysis of the *znf711* promoter revealed multiple putative C/EBPα binding sites (Fig S10). Consistent with direct transcriptional activation, C/ebpα robustly transactivated the *znf711* promoter-luciferase reporter (Fig 8B). Endogenous occupancy of the *znf711* promoter by C/ebpα was confirmed by ChIP-qPCR in zebrafish larvae (Fig 8C). Furthermore, forced *in vivo* expression of *c/ebpα* in the neutrophil lineage significantly upregulated endogenous *znf711* transcripts (Fig 8D).

Thus, we demonstrate that *znf711* is a direct downstream target of C/ebpα. Together with our earlier findings that Znf711 protects *c/ebpα* from repression, this establishes a positive feedback loop. This self-reinforcing circuit ensures a high expression of the master regulator *c/ebpα* at the onset of terminal granulopoiesis, thereby promoting cell differentiation, with subsequent downregulation likely governed by other stage-specific factors.

Discussion

ZNF711 and *PHF8* are linked to XLMR in humans [9,11]. Consistent with this and a prior report in *phf8* morphant zebrafish [16], our *znf711* and *phf8* homozygous mutants also exhibit delayed brain development and craniofacial abnormalities (Fig S11), confirming that zebrafish recapitulate the conserved neurodevelopmental roles of these genes.

Our study further identifies Znf711, Phf8, and Gfi1aa as components of a coherent transcriptional module that ensures the precise expression of the master

regulator *c/ebpα* during terminal granulopoiesis in zebrafish. We demonstrate that the Znf711-Phf8 pair, previously characterized as a transcriptional activator-coactivator complex in other contexts, operates through an unexpected repressive mechanism in neutrophils to fine-tune granulopoiesis.

The dynamic expression of *C/EBPα*, which peaks at the myeloblast and promyelocytes stages and declines upon maturation, is critical for promoting neutrophil development [34,39]. This pattern implies the existence of both permissive and repressive regulatory inputs. While *C/EBPα* can maintain its own expression through auto-regulation [40], it is also a direct repression target of Gfi1aa [35]. Our work identifies Phf8 as a critical negative regulator of this repressive pathway. In the absence of Znf711, Phf8 is released and recruited by Gfi1aa to the *c/ebpα* promoter, where SUMOylated Phf8 functions as a potent corepressor. This mechanism provides a plausible explanation for the loss-of-function ZNF711 mutations and PHF8 amplifications observed in AML patients, suggesting that dysregulation of this pathway may contribute to leukemogenesis.

Our findings reveal a DNA-binding-independent function for Znf711, expanding the known functional repertoire beyond its role as a conventional transcriptional activator in neuronal and other tissues [41]. The ability of both the long and short isoforms of human *ZNF711* to rescue neutrophil development in zebrafish mutants (Fig S12) underscores the physiological relevance and evolutionary conservation of this mechanism.

Similarly, we identify a non-canonical, repressive function for Phf8. While widely recognized as a histone demethylase and transcriptional coactivator, Phf8 can also repress transcription in certain contexts. Previous reports have linked PHF8 to repression through mechanisms involving HDAC1-SIN3A recruitment, association with the repressor protein REST/NRSF, or demethylation of the transcription factor YY1 [31,33,42]. Our work contributes to this emerging paradigm by demonstrating that in neutrophils, Phf8 is recruited by Gfi1aa and requires SUMOylation, but not its

demethylase activity, to repress *c/ebpα*. This suggests that Phf8's repressive function is both context-dependent and mechanistically distinct from its canonical role as an eraser of repressive histone marks.

The dysregulation of PHF8 in hematopoietic malignancies [43], including its amplification in AML and its ability to activate the oncogenic *BCR-ABL1* fusion gene in CML [18], underscores its clinical significance. Furthermore, elevated *PHF8* expression is observed in many types of cancers [42], positioning it as a broad oncogenic driver. Our finding that Phf8 directly represses *c/ebpα*, a gene whose dysfunction is intimately linked to AML, offers a new perspective on its potential oncogenic mechanisms. The Znf711-Phf8-*C/ebpα* regulatory axis we identified in zebrafish may be relevant to human AML, particularly in subtypes with low *ZNF711* expression or *PHF8* amplification. As PHF8 inhibitors are being developed for leukemia and other cancer types [18,42,44], understanding its critical role in normal neutrophil development will be essential for evaluating potential side effects during therapeutic targeting. Finally, our work expands the repertoire of GFI1 corepressors. While GFI1 is well-established as a transcriptional repressor in myelopoiesis and is frequently dysregulated in AML, MDS, and SCN [45,46], its repressive capacity primarily depends on recruitment of the LSD1-CoREST complex [36]. Our data indicate that GFI1 can also recruit Phf8 as an alternative corepressor. Notably, SUMOylation emerges as a common regulatory theme, as it is essential for the repressive activity of GFI1, PHF8, LSD1, and CoREST [47–50], suggesting it may be a general mechanism governing the assembly and function of multi-subunit repressive complexes during myeloid development.

In conclusion, our work delineates a novel circuit in neutrophil development, revealing non-canonical functions for Znf711 and Phf8 and expanding our understanding of the GFI1 repressosome. The conservation of this pathway in humans and its potential dysregulation in leukemia underscore its physiological and clinical importance.

References

1. Dancey JT, Deubelbeiss KA, Harker LA, Finch CA. Neutrophil kinetics in man. J Clin Invest. 1976;58(3):705-715.
2. Yvan-Charvet L, Ng LG. Granulopoiesis and Neutrophil Homeostasis: A Metabolic, Daily Balancing Act. Trends Immunol. 2019;40(7):598-612.
3. Rosenbauer F, Tenen DG. Transcription factors in myeloid development: balancing differentiation with transformation. Nat Rev Immunol. 2007;7(2):105-117.
4. Ai Z, Udalova IA. Transcriptional regulation of neutrophil differentiation and function during inflammation. J Leukoc Biol. 2020;107(3):419-430.
5. Friedman AD. Transcriptional regulation of granulocyte and monocyte development. Oncogene. 2002;21(21):3377-3390.
6. Ostuni R, Natoli G, Cassatella MA, Tamassia N. Epigenetic regulation of neutrophil development and function. Semin Immunol. 2016;28(2):83-93.
7. Kishtagari A, Levine RL, Viny AD. Driver mutations in acute myeloid leukemia. Curr Opin Hematol. 2020;27(2):49-57.
8. Ni W, Perez AA, Schreiner S, Nicolet CM, Farnham PJ. Characterization of the ZFX family of transcription factors that bind downstream of the start site of CpG island promoters. Nucleic Acids Res. 2020;48(11):5986-6000.
9. van der Werf IM, Van Dijck A, Reyniers E, et al. Mutations in two large pedigrees highlight the role of ZNF711 in X-linked intellectual disability. Gene. 2017;605:92-98.
10. Poeta L, Padula A, Attianese B, et al. Histone demethylase KDM5C is a SAHA-sensitive central hub at the crossroads of transcriptional axes involved in multiple neurodevelopmental disorders. Hum Mol Genet. 2019;28(24):4089-4102.
11. Kleine-Kohlbrecher D, Christensen J, Vandamme J, et al. A functional link between the histone demethylase PHF8 and the transcription factor ZNF711 in X-linked mental retardation. Mol Cell. 2010;38(2):165-178.
12. Fagerberg L, Hallström BM, Oksvold P, et al. Analysis of the human tissue-specific expression by genome-wide integration of transcriptomics and antibody-based proteomics. Mol Cell Proteomics. 2014;13(2):397-406.
13. Tyner JW, Tognon CE, Bottomly D, et al. Functional genomic landscape of acute myeloid leukaemia. Nature. 2018;562(7728):526-531.
14. Bienz M. The PHD finger, a nuclear protein-interaction domain. Trends Biochem Sci. 2006;31(1):35-40.
15. Accari SL, Fisher PR. Emerging Roles of JmjC Domain-Containing Proteins. Int Rev Cell Mol Biol. 2015;319:165-220.
16. Qi HH, Sarkissian M, Hu G-Q, et al. Histone H4K20/H3K9 demethylase PHF8 regulates zebrafish brain and craniofacial development. Nature. 2010;466(7305):503-507.
17. Felipe Fumero E, Walter C, Frenz JM, et al. Epigenetic control over the cell-intrinsic immune response antagonizes self-renewal in acute myeloid leukemia. Blood. 2024;143(22):2284-2299.
18. Feng H, Fu Y, Cui Z, et al. Histone demethylase PHF8 facilitates the development of chronic myeloid leukaemia by directly targeting BCR::ABL1. Br J Haematol. 2023;202(6):1178-1191.

19. Hsu K, Kanki JP, Look AT. Zebrafish myelopoiesis and blood cell development. Curr Opin Hematol. 2001;8(4):245-251.
20. Galloway JL, Zon LI. Ontogeny of hematopoiesis: examining the emergence of hematopoietic cells in the vertebrate embryo. Curr Top Dev Biol. 2003;53:139-158.
21. Zon LI. Developmental biology of hematopoiesis. Blood. 1995;86(8):2876-2891.
22. Bertrand JY, Kim AD, Violette EP, Stachura DL, Cisson JL, Traver D. Definitive hematopoiesis initiates through a committed erythromyeloid progenitor in the zebrafish embryo. Development. 2007;134(23):4147-4156.
23. Bertrand JY, Kim AD, Teng S, Traver D. CD41+ cmyb+ precursors colonize the zebrafish pronephros by a novel migration route to initiate adult hematopoiesis. Development. 2008;135(10):1853-1862.
24. Jin H, Huang Z, Chi Y, et al. c-Myb acts in parallel and cooperatively with Cebp1 to regulate neutrophil maturation in zebrafish. Blood. 2016;128(3):415-426.
25. Huang Z, Chen K, Chi Y, et al. Runx1 regulates zebrafish neutrophil maturation via synergistic interaction with c-Myb. J Biol Chem. 2021;296:100272.
26. Theilgaard-Mönch K, Pundhir S, Reckzeh K, et al. Transcription factor-driven coordination of cell cycle exit and lineage-specification in vivo during granulocytic differentiation : In memoriam Professor Niels Borregaard. Nat Commun. 2022;13(1):3595.
27. Savickiene J, Treigyte G, Vistartaite G, Tunaitis V, Magnusson K-E, Navakauskiene R. C/EBPα and PU.1 are involved in distinct differentiation responses of acute promyelocytic leukemia HL-60 and NB4 cells via chromatin remodeling. Differentiation. 2011;81(1):57-67.
28. Pabst T, Mueller BU, Zhang P, et al. Dominant-negative mutations of CEBPA, encoding CCAAT/enhancer binding protein-alpha (C/EBPalpha), in acute myeloid leukemia. Nat Genet. 2001;27(3):263-270.
29. Kooy RF. ZNF711 puts a spell on DNA. Eur J Hum Genet 2022;30(4):396-397.
30. Feng W, Yonezawa M, Ye J, Jenuwein T, Grummt I. PHF8 activates transcription of rRNA genes through H3K4me3 binding and H3K9me1/2 demethylation. Nat Struct Mol Biol. 2010;17(4):445-450.
31. Wang J, Lin X, Wang S, et al. PHF8 and REST/NRSF co-occupy gene promoters to regulate proximal gene expression. Sci Rep. 2014;4:5008.
32. ENCODE Project Consortium. An Integrated Encyclopedia of DNA Elements in the Human Genome. Nature. 2012;489(7414):57-74.
33. Asensio-Juan E, Fueyo R, Pappa S, et al. The histone demethylase PHF8 is a molecular safeguard of the IFNγ response. Nucleic Acids Res. 2017;45(7):3800-3811.
34. Fiedler K, Brunner C. The role of transcription factors in the guidance of granulopoiesis. Am J Blood Res. 2012;2(1):57-65.
35. Wu M, Xu Y, Li J, et al. Genetic and epigenetic orchestration of Gfi1aa-Lsd1-cebpa in zebrafish neutrophil development. Development. 2021;148(17):dev199516.
36. van Bergen MGJM, van der Reijden BA. Targeting the GFI1/1B-CoREST Complex in Acute Myeloid Leukemia. Front Oncol. 2019;9:1027.

37. Gao J, Liu T, Yang D, Tuo Q. The Dynamic Regulation of Daxx-Mediated Transcriptional Inhibition by SUMO and PML NBs. Int J Mol Sci 2025;26(14):6703.
38. Wotton D, Pemberton LF, Merrill-Schools J. SUMO and Chromatin Remodeling. Adv Exp Med Biol. 2017;963:35-50.
39. Xie X, Shi Q, Wu P, et al. Single-cell transcriptome profiling reveals neutrophil heterogeneity in homeostasis and infection. Nat Immunol. 2020;21(9):1119-1133.
40. Christy RJ, Kaestner KH, Geiman DE, Lane MD. CCAAT/enhancer binding protein gene promoter: binding of nuclear factors during differentiation of 3T3-L1 preadipocytes. Proc Natl Acad Sci U S A. 1991;88(6):2593-2597.
41. Rhie SK, Yao L, Luo Z, et al. ZFX acts as a transcriptional activator in multiple types of human tumors by binding downstream from transcription start sites at the majority of CpG island promoters. Genome Res. 2018;28(3):310-320.
42. Wu X-N, Li J-Y, He Q, et al. Targeting the PHF8/YY1 axis suppresses cancer cell growth through modulation of ROS. Proc Natl Acad Sci U S A. 2024;121(2):e2219352120.
43. Fan T, Jiang L, Zhou X, Chi H, Zeng X. Deciphering the dual roles of PHD finger proteins from oncogenic drivers to tumor suppressors. Front Cell Dev Biol. 2024;12:1403396.
44. Fu Y, Yang Y, Wang X, et al. The histone demethylase PHF8 promotes adult acute lymphoblastic leukemia through interaction with the MEK/ERK signaling pathway. Biochem Biophys Res Commun. 2018;496(3):981-987.
45. Möröy T, Khandanpour C. Role of GFI1 in Epigenetic Regulation of MDS and AML Pathogenesis: Mechanisms and Therapeutic Implications. Front Oncol. 2019;9:824.
46. Muench DE, Olsson A, Ferchen K, et al. Mouse models of neutropenia reveal progenitor-stage-specific defects. Nature. 2020;582(7810):109-114.
47. Andrade D, Velinder M, Singer J, et al. SUMOylation Regulates Growth Factor Independence 1 in Transcriptional Control and Hematopoiesis. Mol Cell Biol. 2016;36(10):1438-1450.
48. Rosendorff A, Sakakibara S, Lu S, et al. NXP-2 association with SUMO-2 depends on lysines required for transcriptional repression. Proc Natl Acad Sci U S A. 2006;103(14):5308-5313.
49. Sáez JE, Arredondo C, Rivera C, Andrés ME. PIASγ controls stability and facilitates SUMO-2 conjugation to CoREST family of transcriptional co-repressors. Biochem J. 2018;475(8):1441-1454.
50. Ouyang J, Shi Y, Valin A, Xuan Y, Gill G. Direct binding of CoREST1 to SUMO-2/3 contributes to gene-specific repression by the LSD1/CoREST1/HDAC complex. Mol Cell. 2009;34(2):145-154.

Figure legends

Figure 1. *znf711* deficiency specifically impairs neutrophil development during embryogenesis. (A-K') WISH analyses of neutrophil markers *c/ebp1*, *lyz*, *mpx* from 22 hpf to 5 dpf in wild-type (WT) and *znf711*-deficient zebrafish. Grey boxes and red arrows indicate the main positions of positive cells for each marker in RBI, ICM, VDA, and CHT regions. n/n, the number of embryos/larvae showing representative phenotype/total number of embryos/larvae examined. (L, L') Sudan Black staining in WT and *znf711*-deficient larvae at 48 hpf. (M, M') GFP fluorescence in WT Tg(*mpx*:eGFP) and *znf711*$^{-/-}$//Tg(*mpx*:eGFP) larvae at 48 hpf. (N) Statistical results for A-M' (Student's *t*-test, N = 5, 20-30 embryos/larvae were used for each probe in each experiment. Each dot represents the mean value obtained from all counts within the same group. Error bars represent mean ± SEM. ****P <0.0001). (O) WISH assays of *mpx* in WT embryos injected with *znf711* MO, and *znf711*$^{-/-}$ mutant embryos rescued by WT zebrafish *znf711* or human *ZNF711* mRNA at 48 hpf. (P) Statistical results for O. The statistical significance was calculated by using one-way analysis of variance (ANOVA). N = 5, 25-35 larvae were used for each experiment. Each dot represents the mean value of one experiment. Error bars represent mean ± SEM. ns: not statistically significant, ****P < 0.0001.

Figure 2. Neutrophil impairment persists in adult *znf711*-deficient zebrafish. (A) FACS analysis of GFP positive cells within the myeloid gate of WKMs from one-year-old WT Tg(*mpx*:eGFP) and *znf711*$^{-/-}$//Tg(*mpx*:eGFP) zebrafish. Light scatter and fluorescence profiles of WT and mutant groups in one representative experiment were shown. FSC: forward light scatter, SSC: side light scatter. (B) Statistical results for A. The statistical significance was calculated by using Student's *t*-test, N = 5, each time two WKMs were used in the WT and mutant groups, respectively. Error bars represent mean ± SEM. ****P < 0.0001). (C) May-Grünwald Giemsa staining of *mpx*$^{+}$ neutrophils isolated from the myeloid gate of WT siblings and *znf711*$^{-/-}$//Tg(*mpx*:eGFP) mutants. Scale bar, 5 μm. (D) 300 cytospin-collected *mpx*$^{+}$ cells were

counted on slides. Immature and mature neutrophils were distinguished and quantitated by morphology, and the proportion of mature neutrophils was compared between WT and mutant groups (Student's *t*-test, N = 5. Error bars represent mean ± SEM. ****$P < 0.0001$).

Figure 3. *c/ebpα* downregulation mediates the neutrophil developmental defect in *znf711* mutants. (A) Heatmap displays the expression patterns of key differentially expressed genes in *znf711-deficient* neutrophils versus wild-type cells. (B) Expression of *c/ebpα*, *c/ebp1*, *csf3r*, *mpx*, and *lyz* in GFP positive cells enriched from Tg(*mpx*:eGFP) and *znf711* MO injected Tg(*mpx*:eGFP) larvae at 48 hpf. To determine the relative expression rate, data were normalized to the expression level of WT groups (which were set to 1.0) after normalized to the internal control of *β-actin* (Student's *t*-test, N = 3. Error bars represent mean ± SEM. **$P < 0.01$, ***$P < 0.001$, ****$P < 0.0001$). (C) Rescue assays with the TOL2(*mpx*:*c/ebpα*) plasmid in *znf711*$^{-/-}$ mutants at 48 hpf. Overexpression of *znf711* mRNA in WT embryos in the absence and presence of the TOL2(*mpx*:*c/ebpα*-BZIP) plasmid. *mpx* probe was used in WISH. (D) Statistic result for C. The statistical significance was calculated by using one-way analysis of variance (ANOVA). The asterisk indicates a statistical difference. (N = 5, 23-30 larvae were used for each experiment. Each dot represents the mean value of one experiment. Error bars represent mean ± standard error of the mean (SEM). ns: not statistically significant, ****$P < 0.0001$). (E) RT-qPCR analyses of *c/ebpα* transcripts in *mpx*$^{+}$ cells sorted from WT Tg(*mpx*:eGFP) and WT zebrafish injected with *znf711* mRNA at 48 dpf. Data were normalized to the expression level of WT groups (which were set to 1.0) after normalized to the internal control of *β-actin* (Student's *t*-test, N = 3. Error bars represent mean ± SEM. ****$P < 0.0001$).

Figure 4. Znf711 antagonizes Phf8-mediated repression of *c/ebpα* to promote neutrophil development. (A) WISH assays of *mpx* were conducted in WT, *znf711*$^{-/-}$ mutants, and *znf711*$^{-/-}$ mutants injected with wild-type Znf711, Znf711 ΔZfx/Zfy, and Znf711 ΔDBD mutant mRNAs at 48 hpf. (B) Statistical analysis for A. The statistical

significance was calculated by using one-way ANOVA. The asterisk indicates a statistical difference (N = 5, each experiment used 25-30 larvae. Each dot represents the mean value of one experiment. Error bars represent mean ± SEM. ns: not statistically significant, ****P < 0.0001). (C) Co-IP assays indicated endogenous Znf711 could be immunoprecipitated with an anti-Phf8 antibody in the 32Dcl3 cell line. (D) HA-tagged wild-type Znf711 and Znf711 ΔDBD mutant proteins could both be pulled down by FLAG-tagged Phf8 in HEK293T cells. (E) Dual-luciferase reporter assays. Bars showed the relative luciferase activity on the zebrafish *c/ebpα* promoter (-600 bp ~ -960 bp). Luciferase activities with wild-type *phf8*, shRNA targeting *PHF8*, *phf8* ΔPhd finger mutant, *phf8* ΔJmjC mutant, wild-type *znf711*, *znf711* ΔDBD mutant, wild-type *znf711* and *phf8* coexpression, *znf711* ΔDBD mutant and *phf8* coexpression, were detected and normalized to empty vector $pCS2^{+}$ which was set to 1.0 (Student's *t*-test, N = 3. Error bars represent mean ± SEM. ns: not statistically significant, ****P < 0.0001). (F) ChIP-qPCR analyses of *c/ebpα* promoter in wild-type or *znf711*$^{-/-}$ zebrafish larvae expressing HA-Phf8 by using an anti-HA antibody. Positive: the location of the positive primers. NC: the location of the negative control primers. The statistical significance was calculated by using one-way ANOVA. The asterisk indicates a statistical difference. (N = 3. Error bars represent mean ± SEM. ns: not statistically significant, **P < 0.01, ***P < 0.001).

Figure 5. *znf711* is epistatic to *phf8* in neutrophils. (A) WISH assays of *mpx* in WT and *znf711*$^{-/-}$ mutants injected with *phf8* MO at 48 hpf. (B) Statistic results for G. The statistical significance was calculated by using one-way ANOVA. The asterisk indicates a statistical difference (N = 5, 25-30 larvae were used for each experiment. Each dot represents the mean value of one experiment. Error bars represent mean ± SEM. ns: not statistically significant, ****P < 0.0001). (C) WISH assays of *mpx* in WT, *phf8*$^{-/-}$ mutants, and *phf8*$^{-/-}$ mutants injected with *znf711* MO at 48 hpf. (D) Statistic results for I. The statistical significance was calculated by using one-way ANOVA. The asterisk indicates a statistical difference (N = 5, 20-30 larvae were used for each experiment. Each dot represents the mean value of one experiment. Error bars represent

mean ± SEM. ns: not statistically significant, ****$P < 0.0001$).

Figure 6. Gfi1aa recruits Phf8 to the *c/ebpα* promoter to exert transcriptional repression. (A) Co-IP assays in HEK293T cells coexpressing FLAG-Phf8 and HA-Gfi1aa. (B) Co-IP assays in 32Dcl3 cells where endogenous Phf8 could be immunoprecipitated with an anti-Gfi1 antibody. (C) Dual-luciferase activities on the *c/ebpα* promoter (-600 bp ~ -960 bp) with *gfi1aa* or *phf8* overexpression, *gfi1aa* and *phf8* co-overexpression, shRNA targeting endogenous *GFI1* or *PHF8*, *gfi1aa* overexpression with *PHF8* depletion, and *phf8* overexpression with *GFI1* depletion, were detected and normalized to empty vector $pCS2^{+}$ group which was set to 1.0 (Student's *t*-test, N = 3. Error bars represent mean ± SEM. ns: not statistically significant, *$P < 0.1$, ***$P < 0.001$, ****$P < 0.0001$). (D) ChIP-qPCR analyses of *c/ebpα* promoter in wild-type zebrafish larvae expressing HA-Gfi1aa or HA-Phf8, as well as in *gfi1aa*$^{-/-}$ zebrafish expressing HA-Phf8 by using an anti-HA antibody. Positive: the location of the positive primers. NC: the location of the negative control primers. The statistical significance was calculated by using one-way ANOVA. The asterisk indicates a statistical difference. (N = 3. Error bars represent mean ± SEM. ns: not statistically significant, **$P < 0.01$, ****$P < 0.0001$). (E) WISH assays of *mpx* in WT, *znf711*$^{-/-}$, *znf711*$^{-/-}$ injected with *gfi1aa* MO, *gfi1aa*$^{-/-}$, and *gfi1aa*$^{-/-}$ zebrafish injected with *znf711* MO at 48 hpf. (F) Statistic results for E. The statistical significance was calculated by using one-way ANOVA. The asterisk indicates a statistical difference (N = 5, 20-30 larvae were used for each experiment. Each dot represents the mean value of one experiment. Error bars represent mean ± SEM. ns: not statistically significant, ***$P < 0.001$, ****$P < 0.0001$).

Figure 7. SUMOylation enables Phf8 to function as a transcriptional corepressor. (A) FLAG-tagged WT PHF8 or $PHF8^{K840R}$ mutant was co-expressed with UBC9 along with HA-SUMO1 in HEK293T cells. PHF8 was immunoprecipitated with an anti-FLAG antibody, and detected by western blot with an anti-HA antibody. The red arrow indicates the unmodified form of PHF8, and the blue arrow indicates the SUMOylated

form of PHF8. (B) Dual-luciferase reporter assays. Bars showed the relative luciferase activities of WT, PHF8^{K840R}, and PHF8^{K840R}-SUMO1 fusion on the promoter of zebrafish *c/ebpα* (-600 bp ~ -960 bp). Data were normalized to empty vector pCS2^{+} which was set to 1.0 (Student's *t*-test, N = 3. Error bars represent mean ± SEM. ns: not statistically significant, ****$P < 0.0001$). (C) WISH assays of *mpx* in WT, *phf8*$^{-/-}$, and *phf8*$^{-/-}$ zebrafish injected with TOL2(*mpx*:*PHF8*), TOL2(*mpx*:*PHF8*^{K840R}), and TOL2(*mpx*:*PHF8*^{K840R}-*SUMO1*) plasmids. (D) Statistic results for C. The statistical significance was calculated by using one-way ANOVA. The asterisk indicates a statistical difference (N = 5, 20-30 larvae were used for each experiment. Each dot represents the mean value of one experiment. Error bars represent mean ± SEM. ns: not statistically significant, ****$P < 0.0001$).

Figure 8. *znf711* is a direct downstream target of C/ebpα. (A) 32Dcl3 cells were induced to differentiate into mature neutrophils using ATRA (1 μM for 72 hours). RT-qPCR analyses of the expression levels of endogenous *C/ebpα* and *Znf711* before and after ATRA treatment. *GAPDH* serves as internal control, which was set to 1.0 (Student's *t*-test, N = 3. Error bars represent mean ± SEM. ***$P < 0.001$). (B) Dual-luciferase reporter assays. Bars showed the relative luciferase activity on the promoter of zebrafish *znf711* (-2.0 kb). Luciferase activities with C/ebpα were detected and normalized to empty vector pCS2^{+} which was set to 1.0 (Student's *t*-test, N = 3. Error bars represent mean ± SEM. ****$P < 0.0001$). (C) (Top) Diagram of the *znf711* locus. Two predicted C/EBPα binding sites (JASPAR) within the core promoter region are indicated (triangles). The box denotes the region amplified by ChIP-qPCR. (Bottom) ChIP-qPCR validation of C/ebpα binding to the *znf711* promoter *in vivo*. Enrichment is shown for the region encompassing the predicted sites (Positive) versus a non-specific control (NC). The statistical significance was calculated by using Student's *t*-test. The asterisk indicates a statistical difference. (N = 3. Error bars represent mean ± SEM. ns: not statistically significant, **$P < 0.01$). (D) RT-qPCR analyses of *znf711* in the *mpx*$^{+}$ cells enriched from WT Tg(*mpx*:eGFP) and Tg(*mpx*:eGFP) zebrafish injected with a TOL2(*mpx*:*c/ebpα*) plasmid at 48 hpf. To

determine the relative expression rate, data were normalized to the expression level of WT groups (which were set to 1.0) after normalized to the internal control of *β-actin* (Student's *t*-test, N = 3. Error bars represent mean ± SEM. $^{**}P < 0.01$).

Figure 1

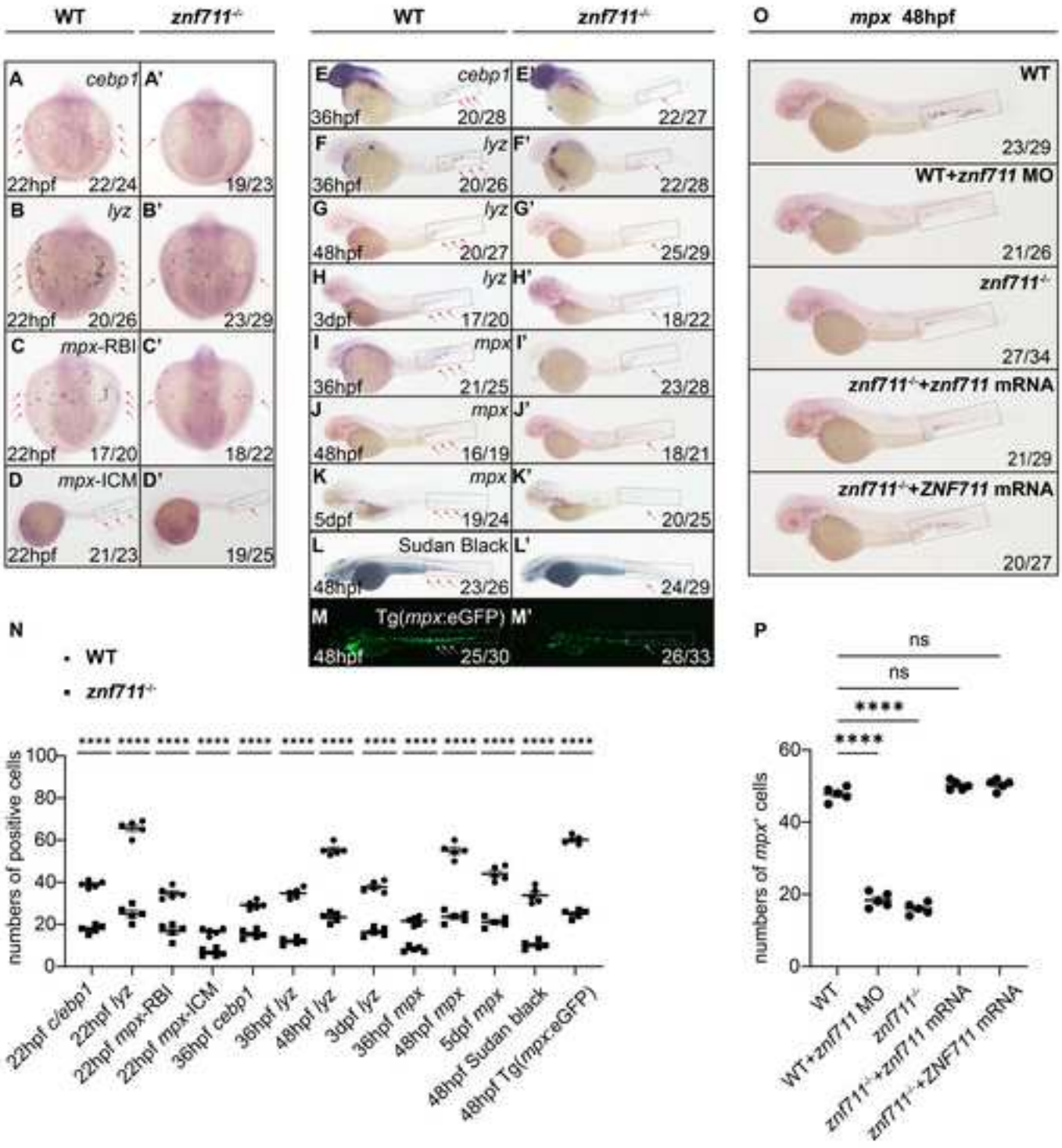
WT
znf711-/-
A cebp1
A'
22hpf 22/24
19/23
B lyz
B'
22hpf 20/26
23/29
C mpx-RBI
C'
22hpf 17/20
18/22
D mpx-ICM
D'
22hpf 21/23
19/25
WT
znf711-/-
E cebp1
E'
36hpf 20/28
22/27
F lyz
F'
36hpf 20/26
22/28
G lyz
G'
48hpf 20/27
25/29
H lyz
H'
3dpf 17/20
18/22
I mpx
I'
36hpf 21/25
23/28
J mpx
J'
48hpf 16/19
18/21
K mpx
K'
5dpf 19/24
20/25
L Sudan Black
L'
48hpf 23/26
24/29
M Tg(mpx:eGFP)
M'
48hpf 25/30
26/33
O mpx 48hpf
WT
23/29
WT+znf711 MO
21/26
znf711-/-
27/34
znf711-/-+znf711 mRNA
21/29
znf711-/-+ZNF711 mRNA
20/27
N
WT
znf711-/-
numbers of positive cells
22hpf cebp1
22hpf lyz
22hpf mpx-RBI
22hpf mpx-ICM
36hpf cebp1
36hpf lyz
48hpf lyz
3dpf lyz
36hpf mpx
48hpf mpx
5dpf mpx
48hpf Sudan black
48hpf Tg(mpx:eGFP)
P
ns
ns
****
****
numbers of mpx+ cells
WT
WT+znf711 MO
znf711-/-
znf711-/-+znf711 mRNA
znf711-/-+ZNF711 mRNA

Figure 2

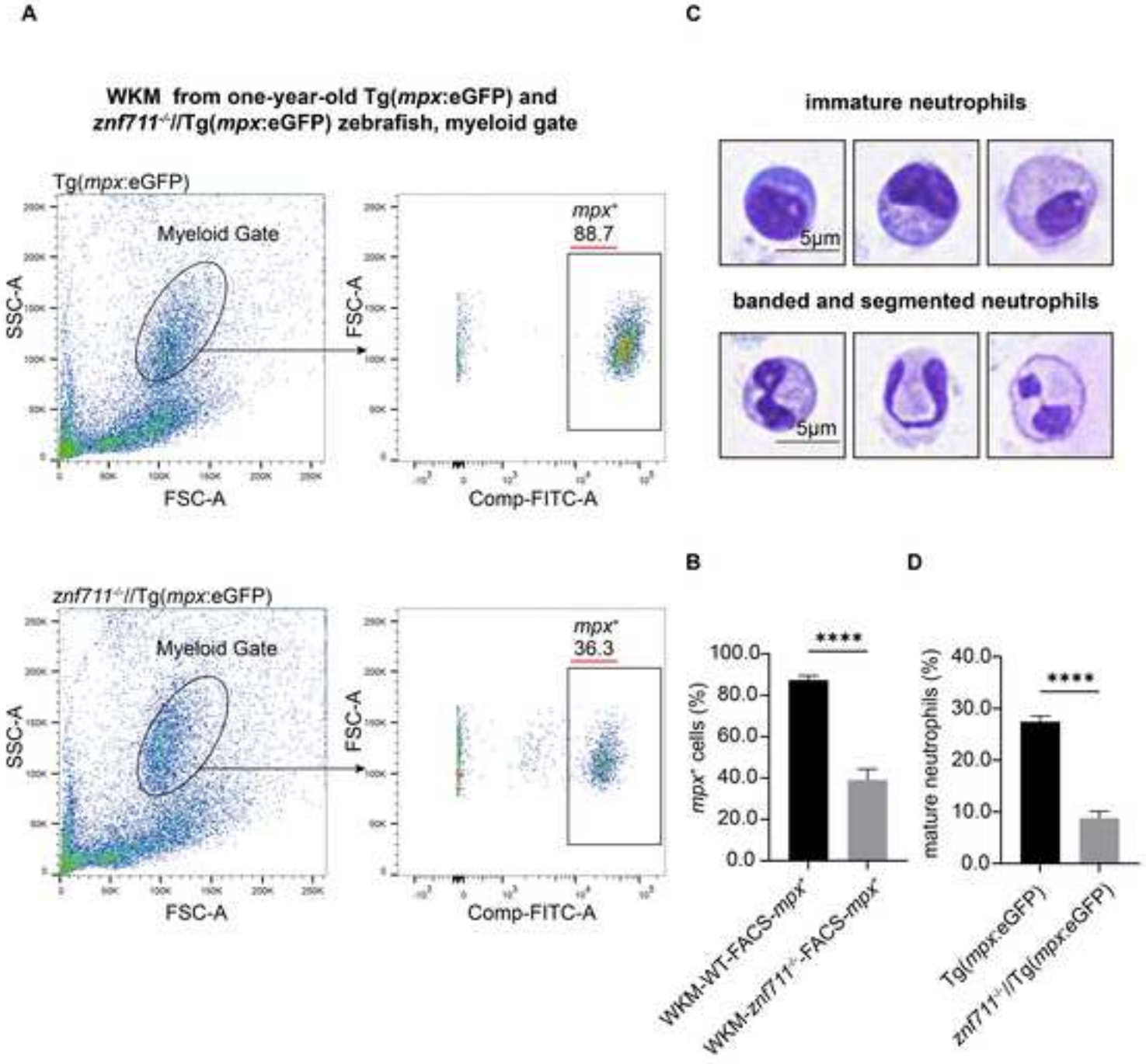
A
WKM from one-year-old Tg(mpx:eGFP) and znf711-/-/Tg(mpx:eGFP) zebrafish, myeloid gate
Tg(mpx:eGFP)
Myeloid Gate
SSC-A
FSC-A
mpx+
88.7
FSC-A
Comp-FITC-A
znf711-/-/Tg(mpx:eGFP)
Myeloid Gate
SSC-A
FSC-A
mpx+
36.3
FSC-A
Comp-FITC-A
C
immature neutrophils
5μm
banded and segmented neutrophils
5μm
B
mpx+ cells (%)
100.0
80.0
60.0
40.0
20.0
0.0
****
WKM-WT-FACS-mpx+
WKM-znf711-/--FACS-mpx+
D
mature neutrophils (%)
40.0
30.0
20.0
10.0
0.0
****
Tg(mpx:eGFP)
znf711-/-/Tg(mpx:eGFP)

Figure 3

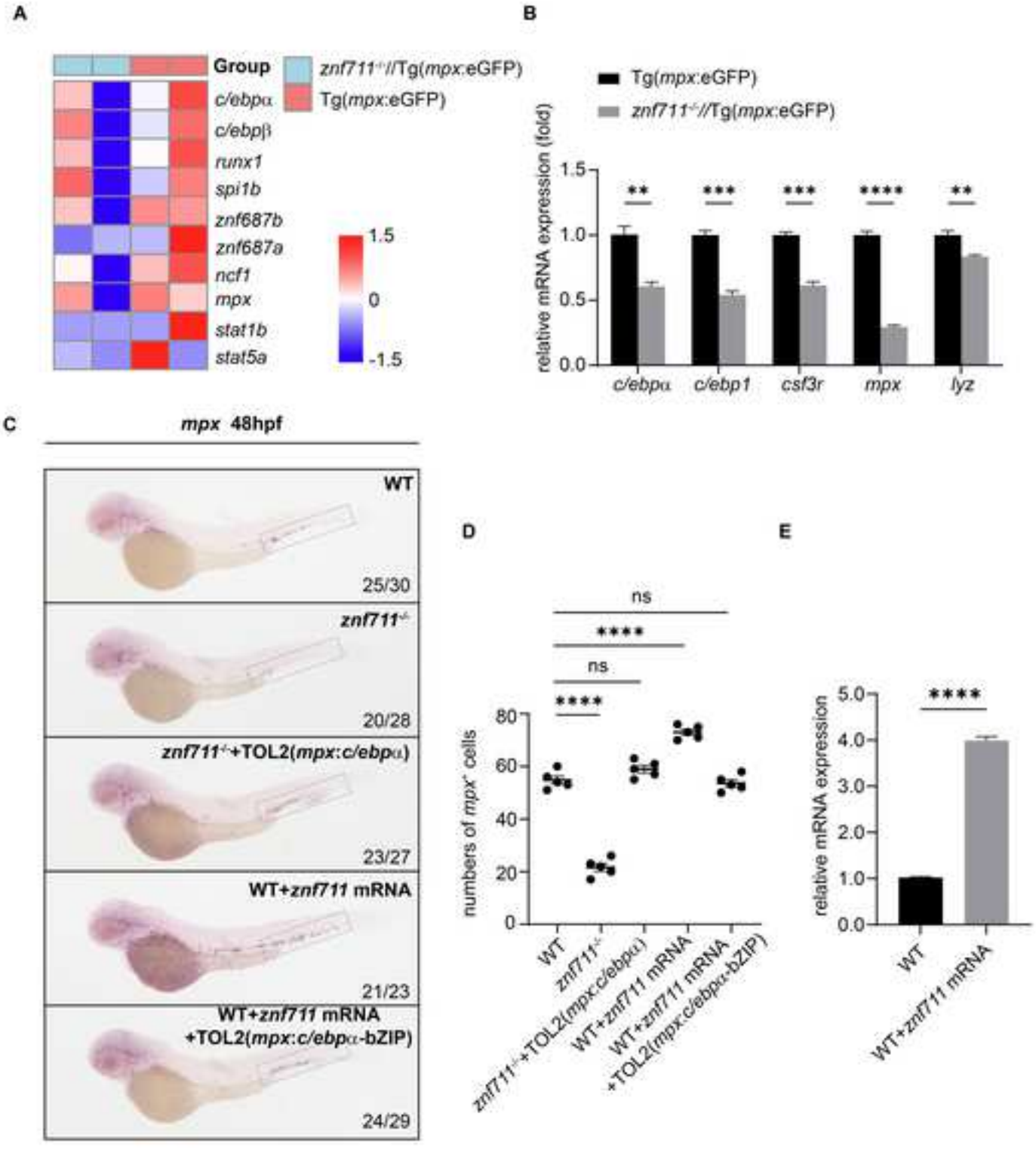
A
Group
znf711-/-//Tg(mpx:eGFP)
Tg(mpx:eGFP)
c/ebpα
c/ebpβ
runx1
spi1b
znf687b
znf687a
ncf1
mpx
stat1b
stat5a
1.5
0
-1.5
B
Tg(mpx:eGFP)
znf711-/-//Tg(mpx:eGFP)
relative mRNA expression (fold)
1.5
1.0
0.5
0.0
**
***
***
****
**
c/ebpα
c/ebp1
csf3r
mpx
lyz
C
mpx 48hpf
WT
25/30
znf711-/-
20/28
znf711-/-+TOL2(mpx:c/ebpα)
23/27
WT+znf711 mRNA
21/23
WT+znf711 mRNA
+TOL2(mpx:c/ebpα-bZIP)
24/29
D
ns
****
ns
****
numbers of mpx+ cells
80
60
40
20
0
WT
znf711-/-
znf711-/-+TOL2(mpx:c/ebpα)
WT+znf711 mRNA
WT+znf711 mRNA
+TOL2(mpx:c/ebpα-bZIP)
E
relative mRNA expression
5.0
4.0
3.0
2.0
1.0
0.0
****
WT
WT+znf711 mRNA

Figure 4

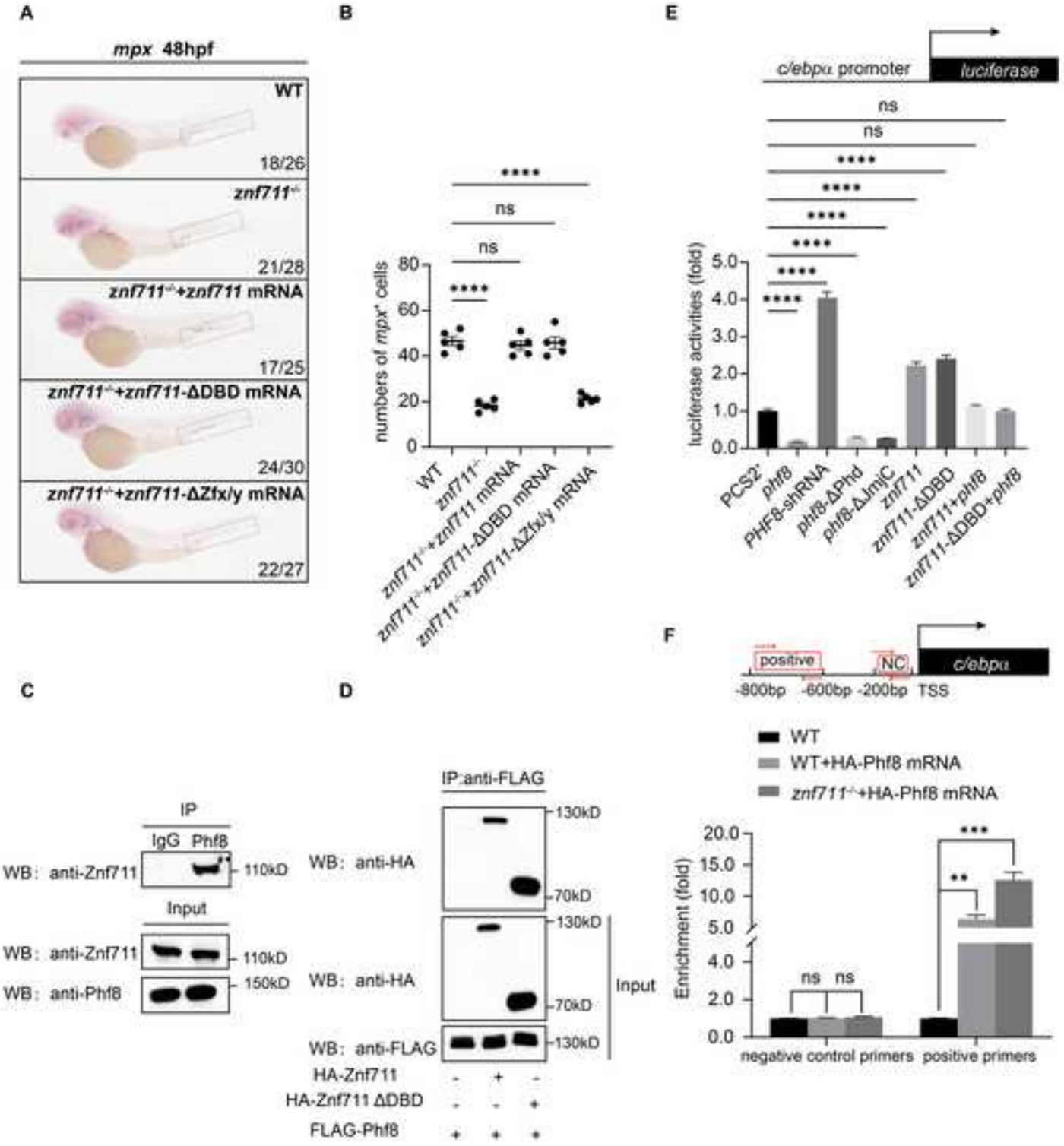
A
mpx 48hpf
WT
18/26
znf711-/-
21/28
znf711-/-+znf711 mRNA
17/25
znf711-/-+znf711-ΔDBD mRNA
24/30
znf711-/-+znf711-ΔZfx/y mRNA
22/27
B
numbers of mpx+ cells
****
ns
ns
****
WT
znf711-/-
znf711-/-+znf711 mRNA
znf711-/-+znf711-ΔDBD mRNA
znf711-/-+znf711-ΔZfx/y mRNA
E
c/ebpα promoter
luciferase
luciferase activities (fold)
PCS2+
phf8
PHF8-shRNA
phf8-ΔPhd
phf8-ΔJmjC
znf711
znf711-ΔDBD
znf711+phf8
znf711-ΔDBD+phf8
C
IP
IgG
Phf8
WB: anti-Znf711
110kD
Input
WB: anti-Znf711
110kD
WB: anti-Phf8
150kD
D
IP:anti-FLAG
WB: anti-HA
130kD
70kD
WB: anti-HA
130kD
70kD
Input
WB: anti-FLAG
130kD
HA-Znf711
HA-Znf711 ΔDBD
FLAG-Phf8
F
positive
NC
c/ebpα
-900bp
-600bp
-200bp
TSS
WT
WT+HA-Phf8 mRNA
znf711-/-+HA-Phf8 mRNA
Enrichment (fold)
***
**
ns
ns
negative control primers
positive primers

Figure 5

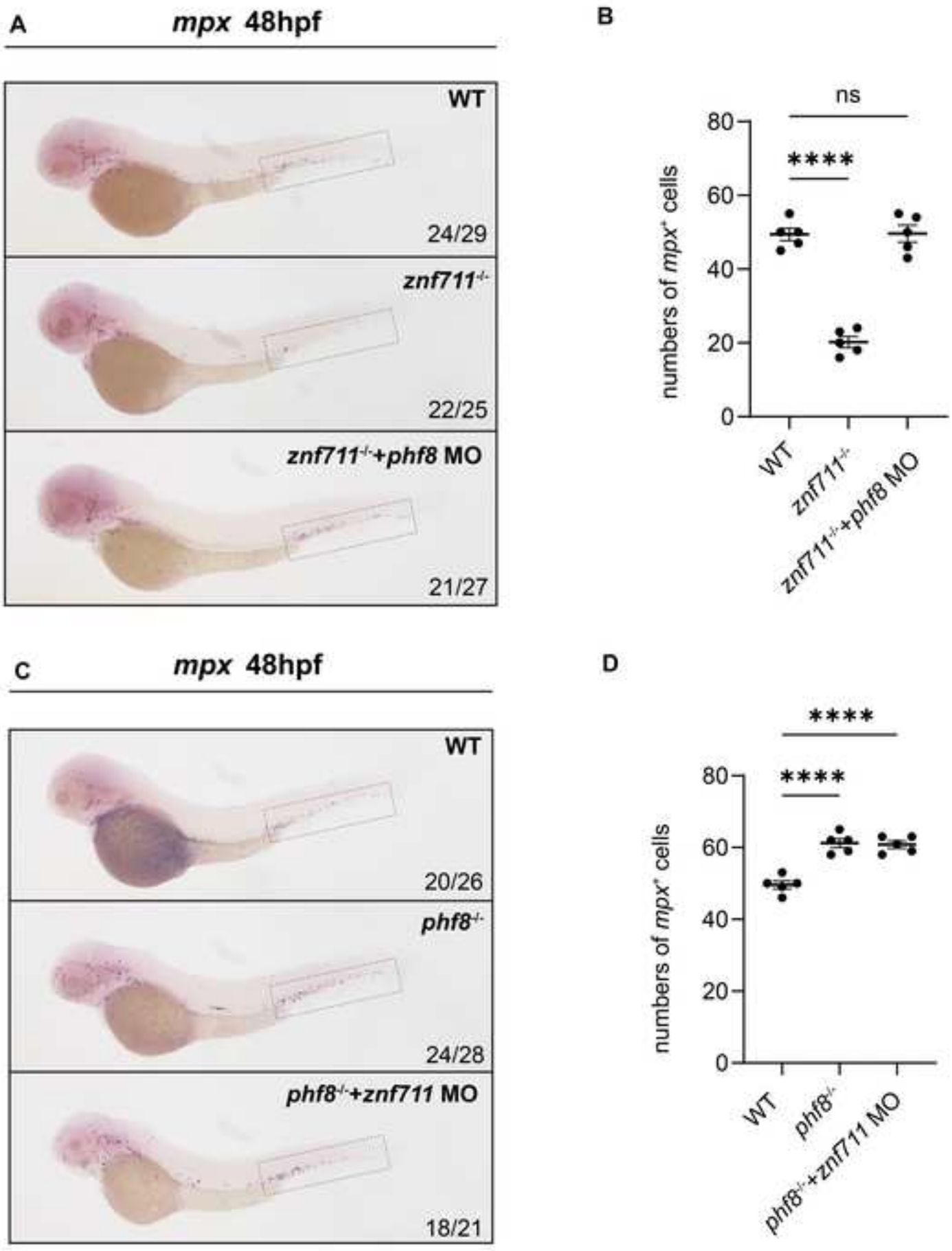
A
mpx 48hpf
WT
24/29
znf711-/-
22/25
znf711-/-+phf8 MO
21/27
B
ns
****
numbers of mpx+ cells
80
60
40
20
0
WT
znf711-/-
znf711-/-+phf8 MO
C
mpx 48hpf
WT
20/26
phf8-/-
24/28
phf8-/-+znf711 MO
18/21
D
****
****
numbers of mpx+ cells
80
60
40
20
0
WT
phf8-/-
phf8-/-+znf711 MO

Figure 6

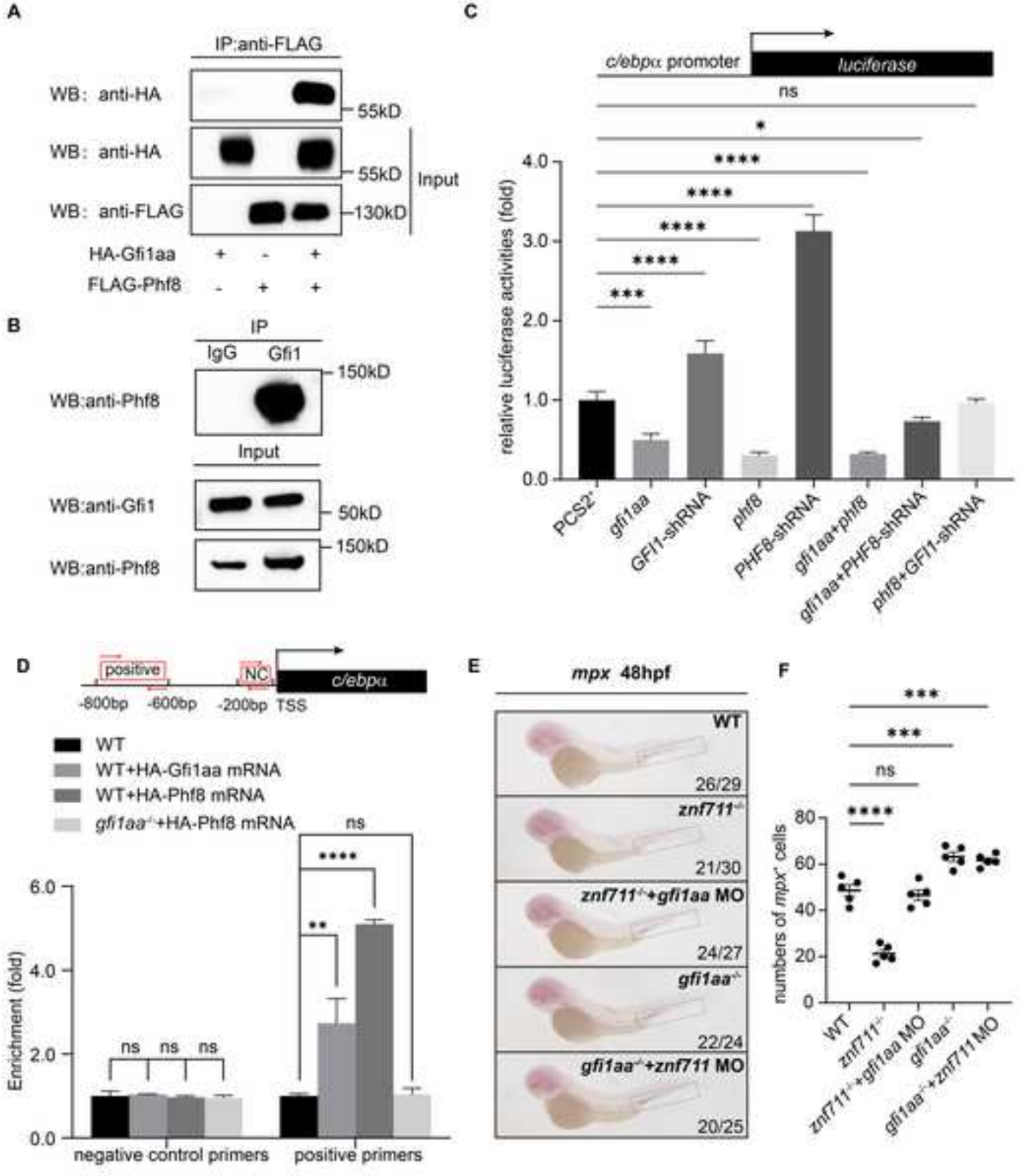
A
IP:anti-FLAG
WB: anti-HA
55kD
WB: anti-HA
55kD
Input
WB: anti-FLAG
130kD
HA-Gfi1aa + - +
FLAG-Phf8 - + +
B
IP
IgG Gfi1
WB:anti-Phf8
150kD
Input
WB:anti-Gfi1
50kD
WB:anti-Phf8
150kD
C
c/ebpα promoter
luciferase
ns
*
****
****
****
****
***
relative luciferase activities (fold)
4.0
3.0
2.0
1.0
0.0
PCS2+
gfi1aa
GFI1-shRNA
phf8
PHF8-shRNA
gfi1aa+phf8
gfi1aa+PHF8-shRNA
phf8+GFI1-shRNA
D
positive
NC
c/ebpα
-800bp -600bp -200bp TSS
WT
WT+HA-Gfi1aa mRNA
WT+HA-Phf8 mRNA
gfi1aa-/-+HA-Phf8 mRNA
Enrichment (fold)
6.0
4.0
2.0
0.0
ns ns ns
ns
****
**
negative control primers
positive primers
E
mpx 48hpf
WT
26/29
znf711-/-
21/30
znf711-/-+gfi1aa MO
24/27
gfi1aa-/-
22/24
gfi1aa-/-+znf711 MO
20/25
F
***
***
ns
****
numbers of mpx+ cells
80
60
40
20
0
WT
znf711-/-
znf711-/-+gfi1aa MO
gfi1aa-/-
gfi1aa-/-+znf711 MO

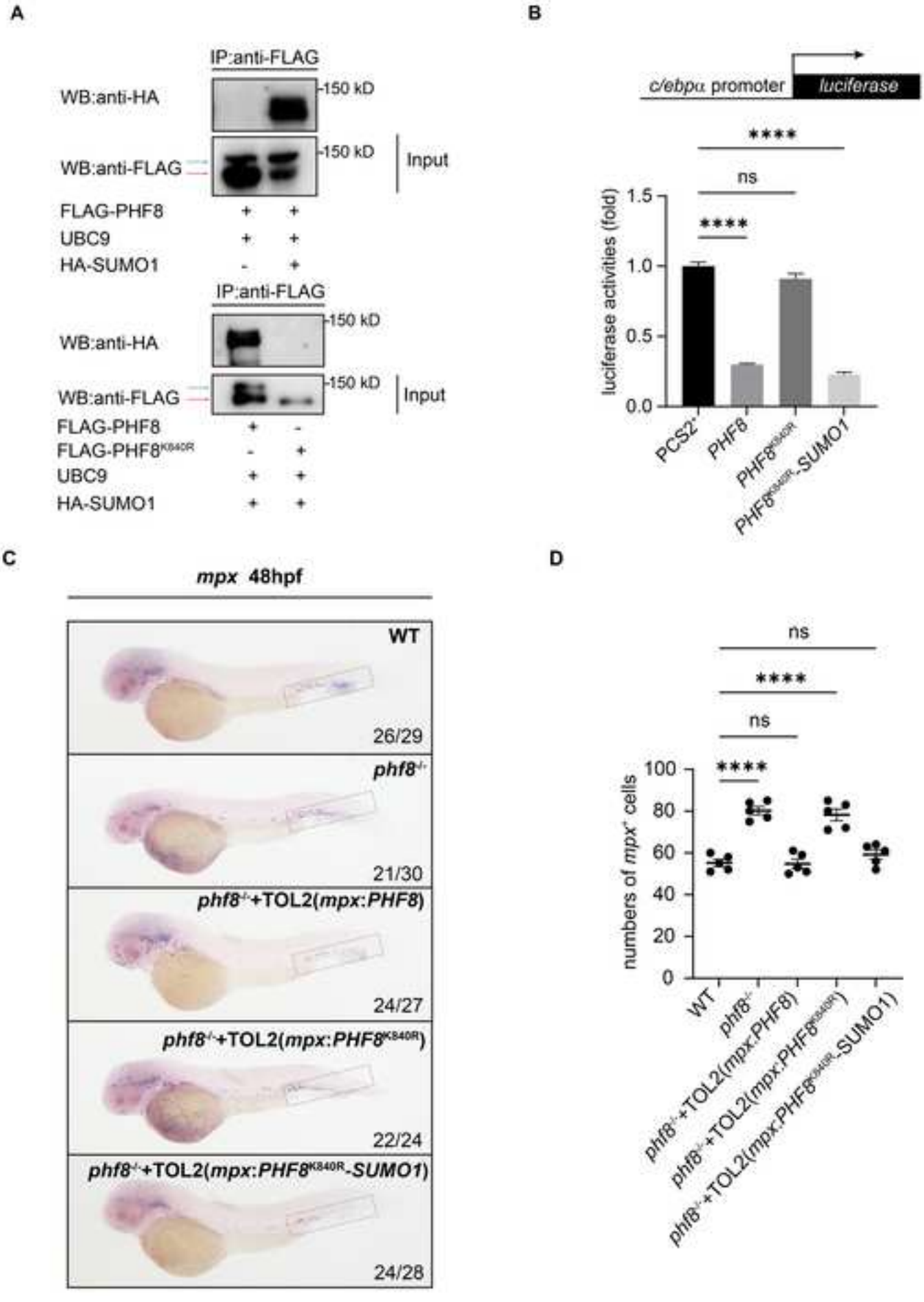
A
IP:anti-FLAG
WB:anti-HA
150 kD
WB:anti-FLAG
150 kD
Input
FLAG-PHF8 + +
UBC9 + +
HA-SUMO1 - +
IP:anti-FLAG
WB:anti-HA
150 kD
WB:anti-FLAG
150 kD
Input
FLAG-PHF8 + -
FLAG-PHF8K840R - +
UBC9 + +
HA-SUMO1 + +
B
c/ebpα promoter
luciferase
****
ns
****
luciferase activities (fold)
1.5
1.0
0.5
0.0
PCS2+
PHF8
PHF8K840R
PHF8K840R-SUMO1
C
mpx 48hpf
WT
26/29
phf8-/-
21/30
phf8-/-+TOL2(mpx:PHF8)
24/27
phf8-/-+TOL2(mpx:PHF8K840R)
22/24
phf8-/-+TOL2(mpx:PHF8K840R-SUMO1)
24/28
D
ns
****
ns
****
numbers of mpx+ cells
100
80
60
40
20
0
WT
phf8-/-
phf8-/-+TOL2(mpx:PHF8)
phf8-/-+TOL2(mpx:PHF8K840R)
phf8-/-+TOL2(mpx:PHF8K840R-SUMO1)

Figure 8

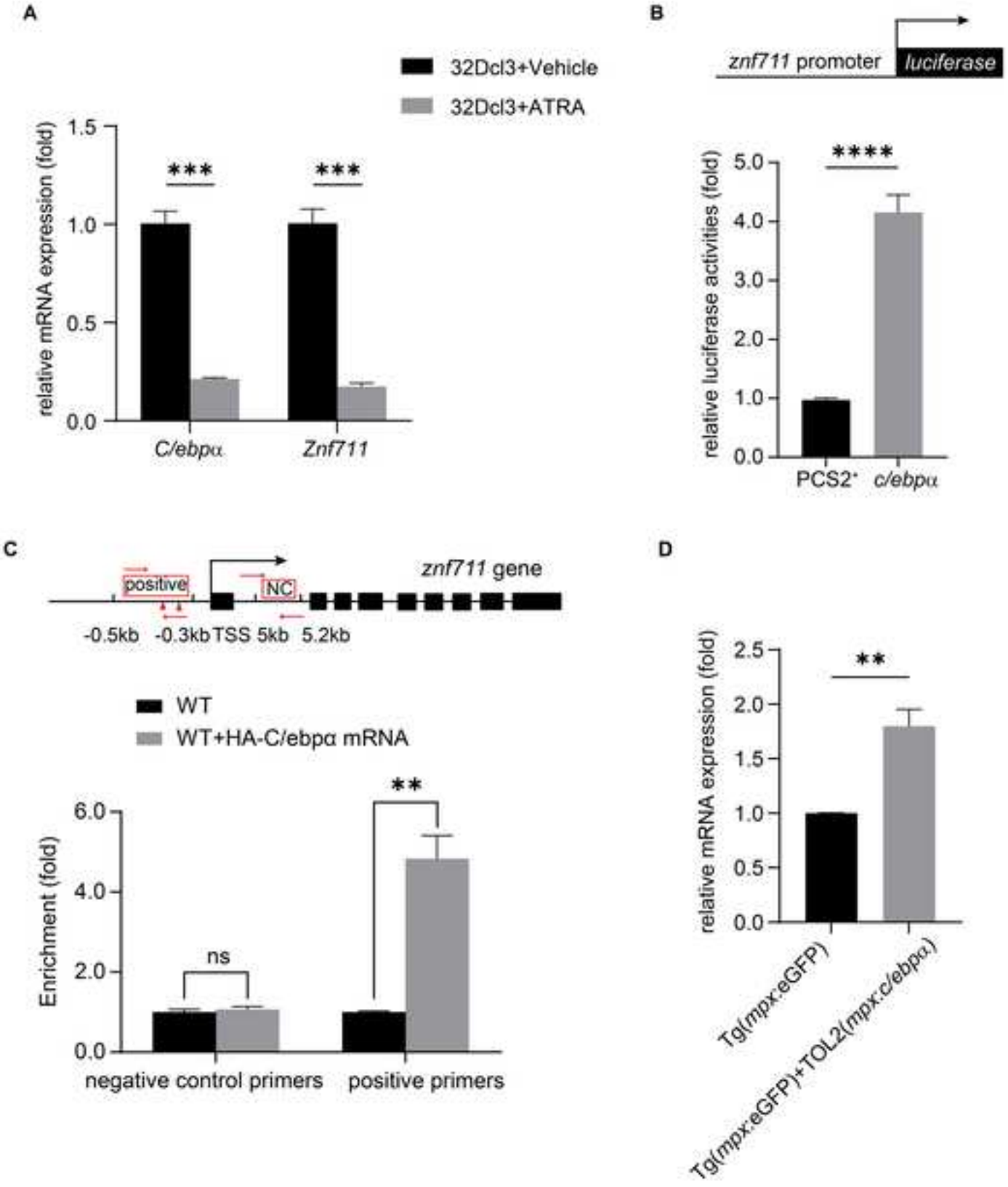
A
32Dcl3+Vehicle
32Dcl3+ATRA
relative mRNA expression (fold)
1.5
1.0
0.5
0.0
***
***
C/ebpα
Znf711
B
znf711 promoter
luciferase
relative luciferase activities (fold)
5.0
4.0
3.0
2.0
1.0
0.0
****
PCS2*
c/ebpα
C
znf711 gene
positive
NC
-0.5kb
-0.3kb
TSS
5kb
5.2kb
WT
WT+HA-C/ebpα mRNA
Enrichment (fold)
6.0
4.0
2.0
0.0
**
ns
negative control primers
positive primers
D
relative mRNA expression (fold)
2.5
2.0
1.5
1.0
0.5
0.0
**
Tg(mpx:eGFP)
Tg(mpx:eGFP)+TOL2(mpx:c/ebpα)

Supplemental Information

Supplemental Figures and Figure legends

Figure S1. Expression and mutation landscape of *ZNF711* in normal granulopoiesis and AML. (A) Expression of *ZNF711* during normal human granulopoiesis and in AML subtypes (the BloodSpot database). *ZNF711* expression peaks in early neutrophils and declines with terminal differentiation (blue box). In most AML subtypes, *ZNF711* expression is lower compared to normal controls, except in t(15;17) acute promyelocytic leukemia (red box). (B) Spectrum of *ZNF711* mutations in five AML patients (the BeatAML database).

A

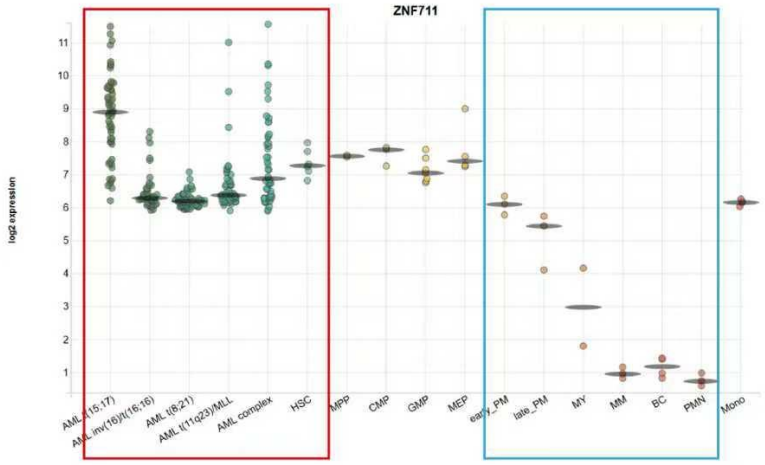

Abbreviation	Name	Immunophenotype
AML t(15;17)	AML with t(15;17)	Whole BM unsorted
AML inv(16)/t(16;16)	AML with inv(16)/t(16;16)	Whole BM unsorted
AML t(8;21)	AML with t(8;21)	Whole BM unsorted
AML t(11q23)/MLL	AML with t(11q23)/MLL	Whole BM unsorted
AML complex	AML with complex aberrant karyotype	Whole BM unsorted
HSC	Hematopoietic stem cell	Lin- CD34+ CD38- CD90+ CD45RA-
MPP	Multipotential progenitors	Lin- CD34+ CD38- CD90- 45RA-
CMP	Common myeloid progenitor cell	Lin- CD34+ CD38+ CD45RA- CD123+
GMP	Granulocyte monocyte progenitors	Lin- CD34+ CD38+ CD45RA+ CD123+
MEP	Megakaryocyte-erythroid progenitor cell	Lin- CD34+ CD38+ CD45RA- CD123-
early_PM	Early Promyelocyte	Lin- FSChi SSCint CD34- CD15int CD49dhi CD33hi CD11b- CD16-
late_PM	Late Promyelocyte	Lin- FSChi SSChi CD34- CD15hi CD49dhi CD33hi CD11b- CD16-
MY	Myelocyte	Lin- FSChi SSChi CD34- CD15hi CD49dhi CD33hi CD11bhi CD16-
MM	Metamyelocytes	Lin- FSChi SSChi CD34- CD15hi CD49d- CD33- CD11bhi CD16-
BC	Band cell	Lin- FSChi SSChi CD34- CD15hi CD49d- CD33- CD11bhi CD16int
PMN	Polymorphonuclear cells	Lin- FSChi SSChi CD34- CD15hi CD49d- CD33- CD11bhi CD16hi
Mono	Monocytes	CD14+ CD16-

B

Patients with variants in ZNF711 (Chr X: 84523336-84523336)

Export

Patient ▲	Sample	Transcript	Variant classification	Amino acids	Protein position
2094	BA2728	ENST00000373165	missense_variant	C/F	318/761
2408	BA2193	ENST00000373165	missense_variant	C/F	318/761
2408	BA2193	ENST00000373165	missense_variant	A/S	320/761
2430	BA2652	ENST00000373165	missense_variant	C/F	318/761
2467	BA2047	ENST00000373165	start_stop_gain_loss_variant	E/*	316/761
2555	BA2284	ENST00000373165	missense_variant	C/F	318/761

Figure S2. Sequence alignment analysis of human ZNF711 and zebrafish Znf711. (A) Their Zfx/Zfy transcription activation regions and consecutive zinc finger domains are highly conserved. Hs: Homo sapiens, Dr: Danio rerio.

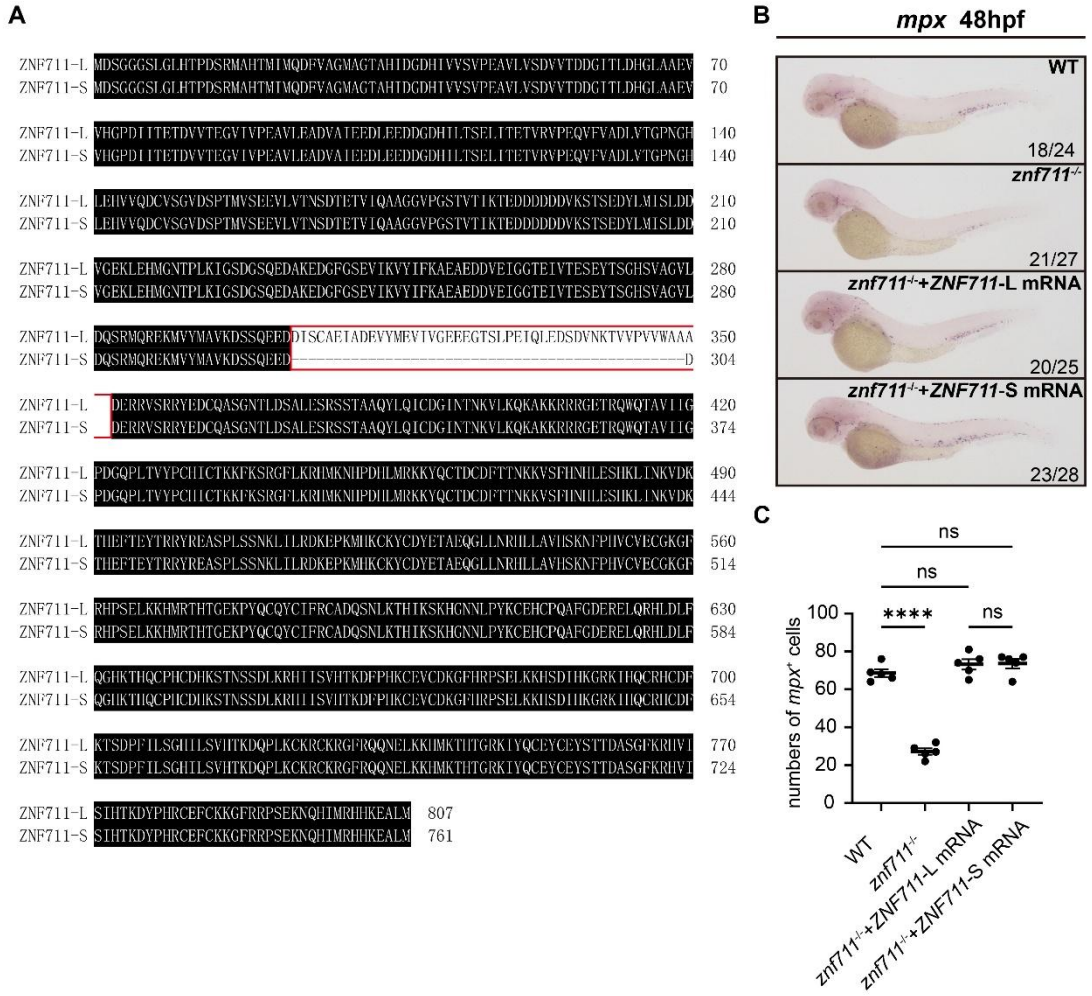

Figure S3. Generation of a *znf711*-deficient zebrafish line. (A, B) Schematic representation of the Cas9 target site in the fourth exon of the *znf711* gene. The deleted nucleotides in the mutant gene are marked by hyphens. Schematic representation of the wild-type (761 aa) and mutant Znf711 proteins (29 aa). Dr: Danio rerio. (C) RT-qPCR data confirmed the significant reduction of *znf711* transcripts in the homozygous mutants. To determine the relative expression rate, data were normalized to the expression level of WT groups (which were set to 1.0) after normalized to the internal control of *β-actin* (Student's *t*-test, N = 3. Error bars represent mean ± SEM. ****$P < 0.0001$).

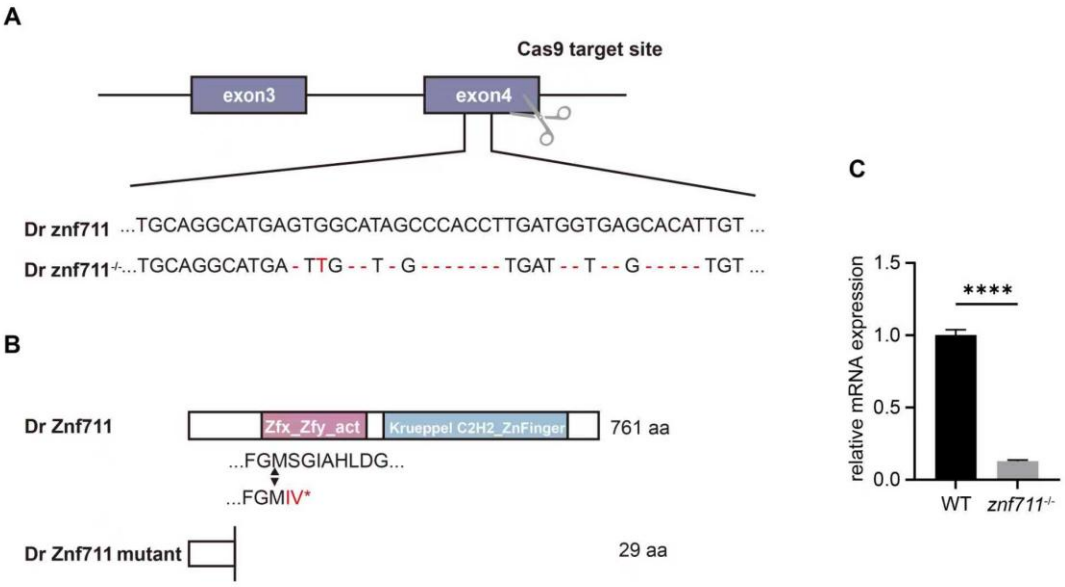

Figure S4. Expression of lineage-specific markers during primitive and definitive hematopoiesis stages in *znf711*-deficient embryos and larvae. (A-D') WISH analyses of hematopoietic progenitor marker *scl*, erythroid markers *gata1*, *hbae1*, macrophage marker *mfap4* in ICM and RBI at 22 hpf. (E-I') WISH analyses of HSPCs marker *c-myb*, macrophage markers *mfap4* and *csf1ra*, erythroid marker *hbae1*, lymphoid marker *rag1* in VDA and CHT during definitive stage of hematopoiesis. (J) Neutral red staining (NR) to detect macrophages at 72 hpf. (K) O-diansidine staining to detect hemoglobin-containing cells at 72 hpf. (L) Statistical results for A-K' (Student's *t*-test, N = 5, 18-35 embryos/larvae were used for each probe. Each dot represents the mean value of one experiment, which was obtained from the counts of all of the embryos/larvae in the same group. ns: not statistically significant).

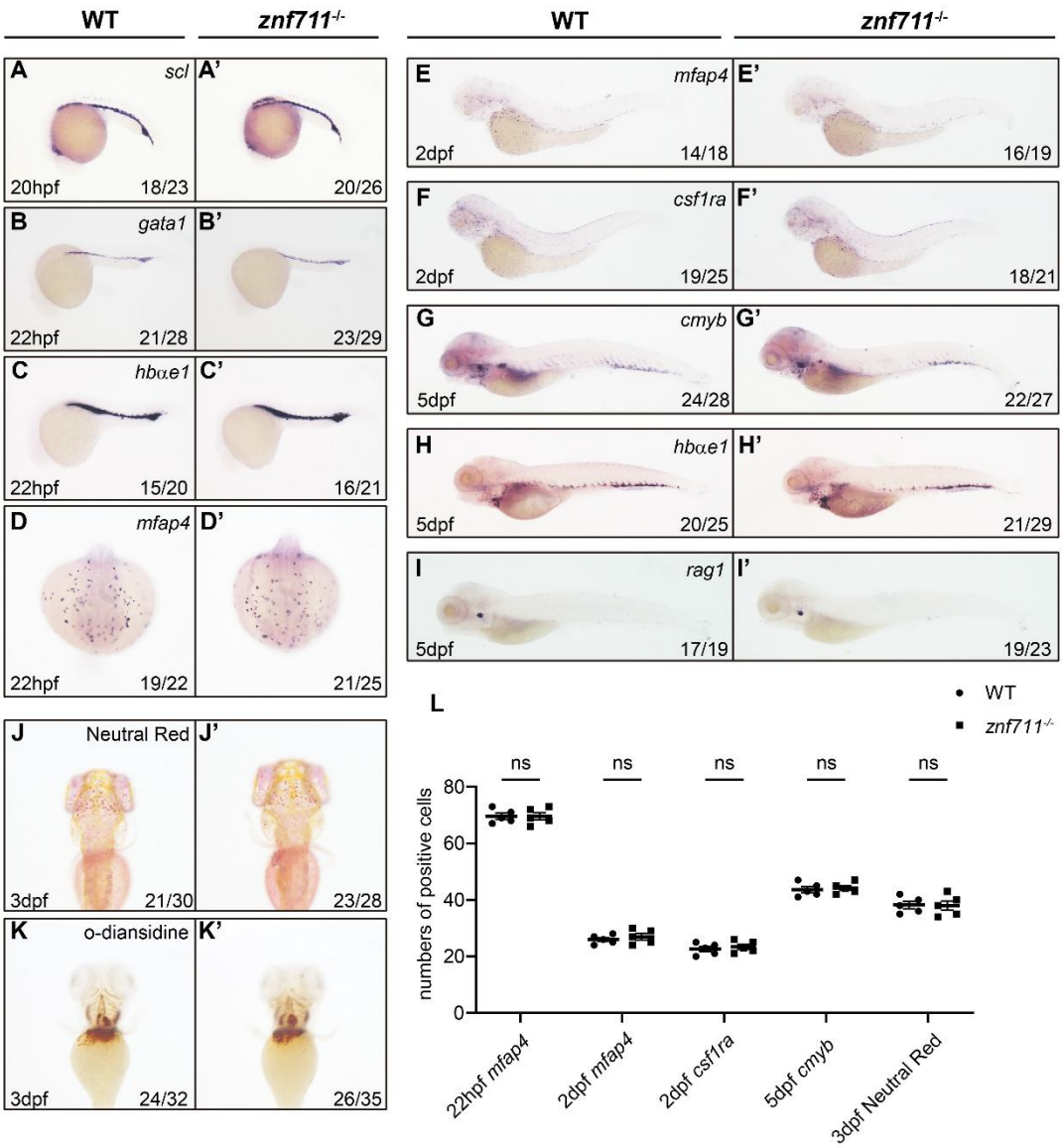
WT
znf711-/-
A scl
A'
20hpf 18/23
20/26
B gata1
B'
22hpf 21/28
23/29
C hbαe1
C'
22hpf 15/20
16/21
D mfap4
D'
22hpf 19/22
21/25
J Neutral Red
J'
3dpf 21/30
23/28
K o-diansidine
K'
3dpf 24/32
26/35
WT
znf711-/-
E mfap4
E'
2dpf 14/18
16/19
F csf1ra
F'
2dpf 19/25
18/21
G cmyb
G'
5dpf 24/28
22/27
H hbαe1
H'
5dpf 20/25
21/29
I rag1
I'
5dpf 17/19
19/23
L
WT
znf711-/-
ns
numbers of positive cells
80
60
40
20
0
22hpf mfap4
2dpf mfap4
2dpf csf1ra
5dpf cmyb
3dpf Neutral Red

Figure S5. The percentages of cells in the erythrocyte and lymphocyte gates were comparable between WT and *znf711*-deficient mutants. FACS analysis of the erythrocyte and lymphocyte gates of WKMs from one-year-old WT and *znf711*$^{-/-}$ zebrafish. Light scatter profiles of WT and mutant groups in one representative experiment were shown. FSC: forward light scatter, SSC: side light scatter. (B) Statistical results for A. The statistical significance was calculated by using Student's *t*-test, N = 5, each time two WKMs were used in the WT and mutant groups, respectively. Error bars represent mean ± SEM. ns: not statistically significant).

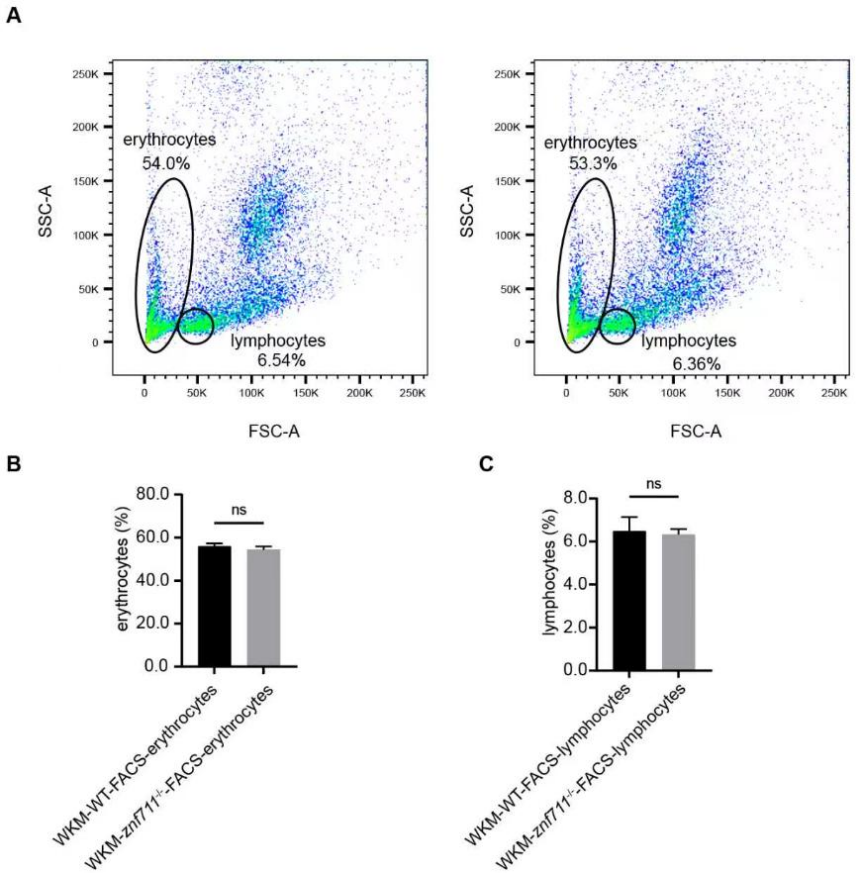

Figure S6. PHF8 occupancy at the *C/EBPα* promoter in human myeloid cell line K562 (data from the Cistrome website).

A

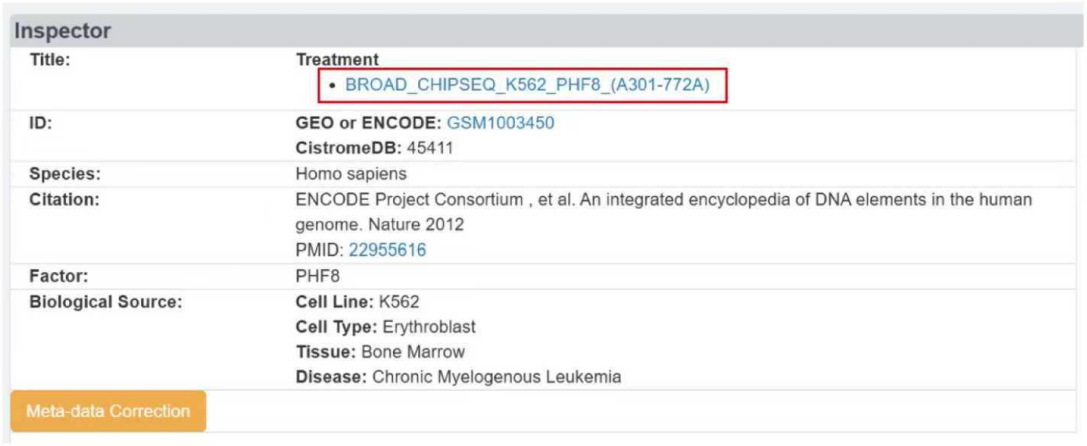

B

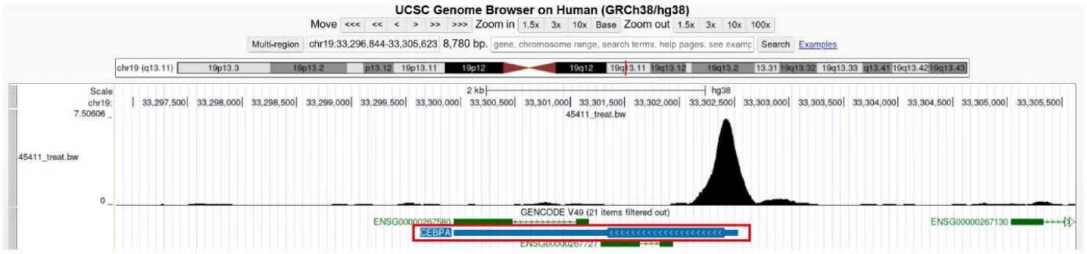

Figure S7. Generation of a *phf8*-deficient zebrafish line. (A, B) Schematic representation of the Cas9 target site in the exon 5 of the *phf8* gene. The deleted nucleotides in the mutant gene are marked by hyphens. Schematic representation of the wild-type (1032 aa) and mutant Phf8 proteins (155 aa). Dr: Danio rerio. (C) RT-qPCR data confirmed the significant reduction of *phf8* transcripts in the homozygous mutants. To determine the relative expression rate, data were normalized to the expression level of WT groups (which were set to 1.0) after normalized to the internal control of *β-actin* (Student's *t*-test, N = 3. Error bars represent mean ± SEM. ****$P < 0.0001$).

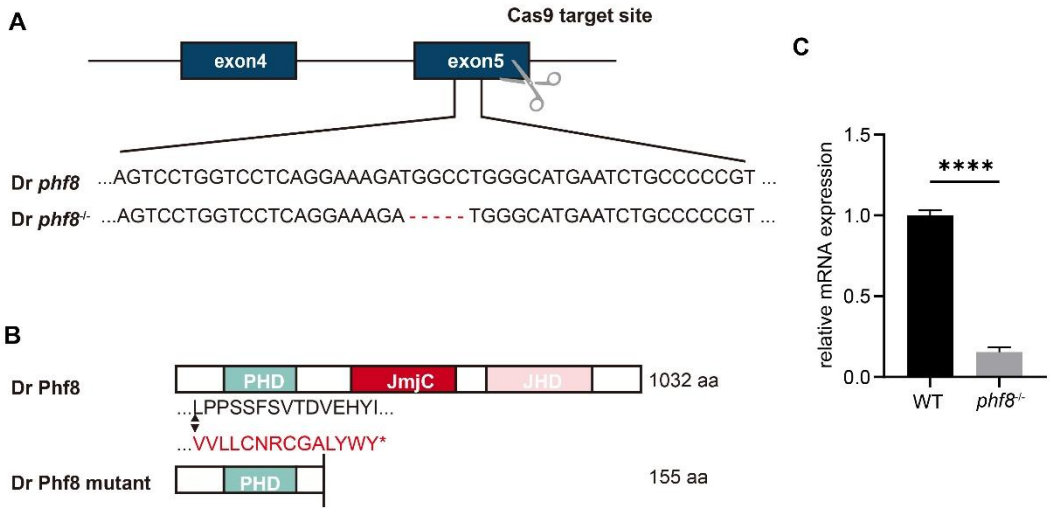

Figure S8. Quantification of indicated transcripts. (A) RT-qPCR analyses of *c/ebpα* in the *mpx*$^{+}$ cells enriched from WT and *phf8*$^{-/-}$//Tg(*mpx*:eGFP) zebrafish larvae at 48 dpf. To determine the relative expression rate, data were normalized to the expression level of WT groups (which were set to 1.0) after normalized to the internal control of *β-actin* (Student's *t*-test, N = 3. Error bars represent mean ± SEM. ****$P < 0.0001$). (B) RT-qPCR analyses of *gfi1aa* transcripts in WT and *gfi1aa*$^{-/-}$ zebrafish larvae at 48 dpf. Data were normalized to the expression level of WT groups (which were set to 1.0) after normalized to the internal control of *β-actin* (Student's *t*-test, N = 3. Error bars represent mean ± SEM. ****$P < 0.0001$). To determine the relative expression rate, data were normalized to the expression level of WT groups (which were set to 1.0) after normalized to the internal control of *β-actin* (Student's *t*-test, N = 3. Error bars represent mean ± SEM. **$P < 0.01$).

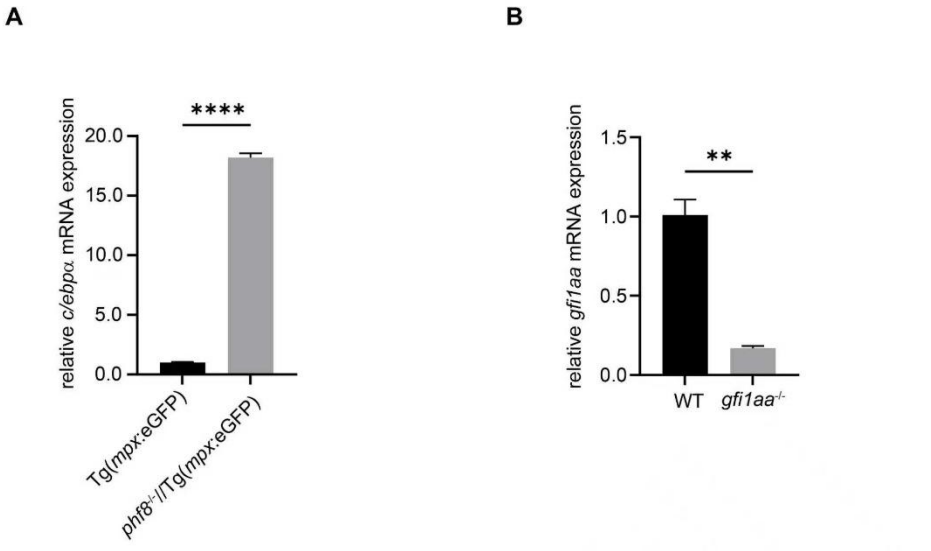

Figure S9. Co-IP assays of the components forming the GFI1-LSD1-RCOR1 complexes in the presence and absence of PHF8. (A, B) Co-IP assays indicated that HA-GFI1 could interact with FLAG-LSD1 and FLAG-RCOR1 in HEK293T cells. Upon silencing of endogenous *PHF8*, the interactions between GFI1 and the other two components were not affected.

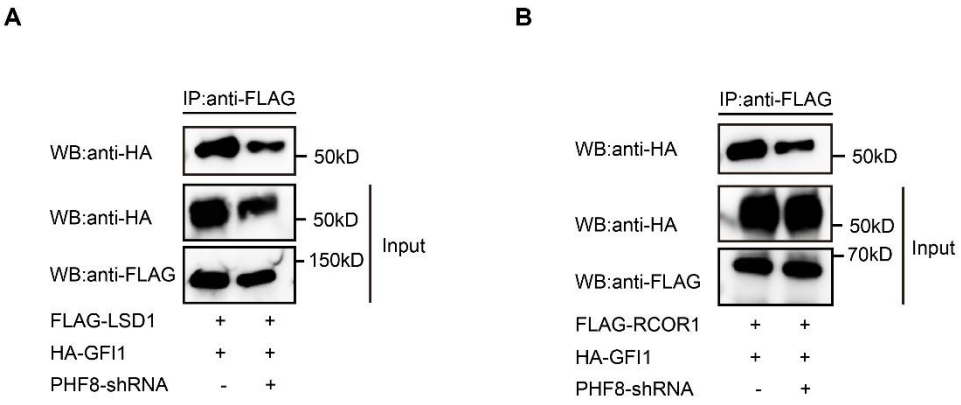

Figure S10. Prediction of C/EBPα binding sites in the *znf711* promoter. (A) Four putative C/EBPα binding sites were predicted in the -2.0 kb upstream region using JASPAR. Two sites within the core promoter (red boxes) were validated by ChIP-qPCR.

Fig S10

A

Analysis results

Scan results

Total **4** putative site(s) were predicted with relative profile score threshold 90%.

Show FASTA Sequence

Display 10 profiles Filter:

Matrix ID	Name	Score	Relative score	Sequence ID		Start	End	Strand	Predicted sequence
MA0102.3	MA0102.3.CEBPA	12.594508	0.9488727	1	-0.3kb	1691	1701	-	ATTGCCTAACA
MA0102.3	MA0102.3.CEBPA	11.274717	0.93306154	1		1159	1169	-	GTTTCACAAGC
MA0102.3	MA0102.3.CEBPA	9.760794	0.91492456	1		188	198	-	GTTTCAAAAGC
MA0102.5	MA0102.5.CEBPA	11.5849	0.90014446	1	-0.36kb	1634	1643	-	ATTGCACATT

Showing 1 to 4 of 4 entries Previous 1 Next

Figure S11. Both *znf711*- and *phf8*-deficient zebrafish displayed brain and craniofacial developmental abnormalities. (A, B) Brain and craniofacial development were delayed at 24 hpf and 7 dpf in both lines.

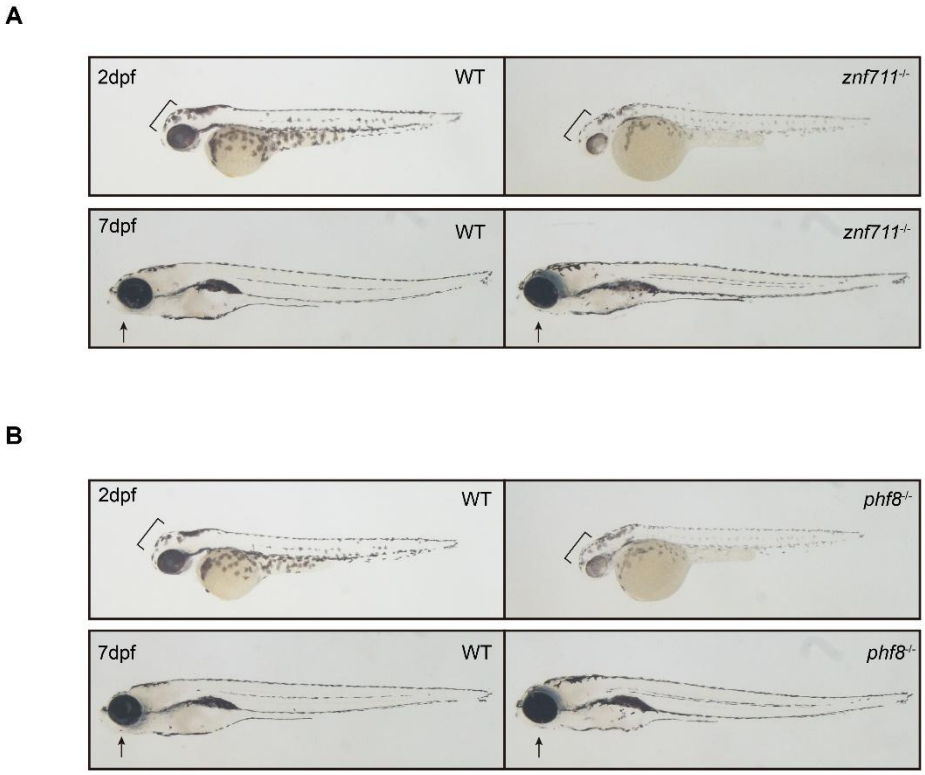

Figure S12. *in vivo* mRNA rescue assays with the long and short isoforms of human *ZNF711*. (A) Human ZNF711 has two isoforms generated through alternative splicing. They differ in 46 amino acid residues within the Zfx/Zfy region (the boxed area). ZNF711-L: the long isoform of ZNF711, ZNF711-S: the short isoform of ZNF711. (B) WISH assays of *mpx* conducted in *znf711*$^{-/-}$ mutants injected with the long or short isoforms of human *ZNF711* mRNA at 48 hpf. (C) Statistic results for B. The statistical significance was calculated by using one-way ANOVA. The asterisk indicates a statistical difference (N = 5, 25-30 larvae were used for each experiment. Each dot represents the mean value of one experiment. Error bars represent mean ± SEM. ns: not statistically significant, ****$P < 0.0001$).

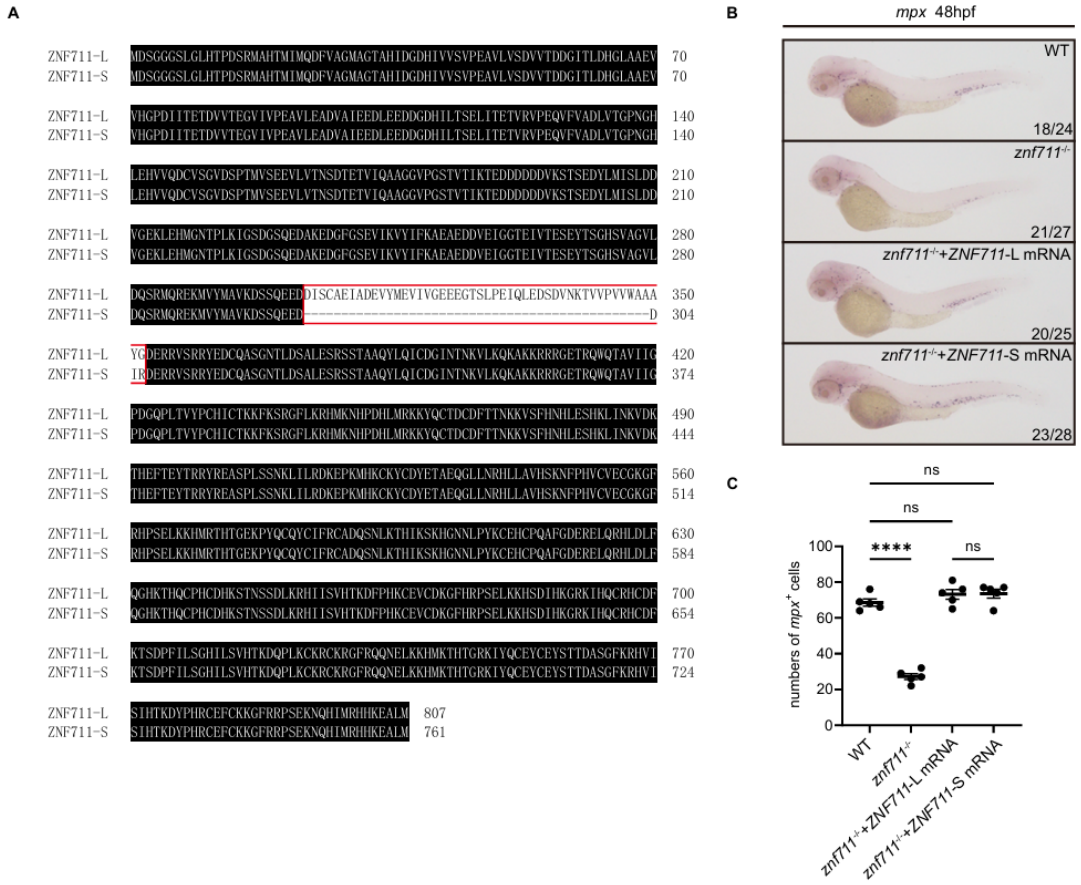

Table S1. Primers used in this study.

Primers for real-time RT-qPCR

Species	**Gene**	**Forward (5'-3')**	**Reverse (5'-3')**
Danio rerio	*β-actin*	TGCTGTTTTCCCCTCCATTG	TTCTGTCCCATGCCAACCA
Danio rerio	*c/ebpα*	TGAAGATTGGCGATCGAGGG	ATTTTCGCCTTGTCCCGACT
Danio rerio	*c/ebp1*	TCTGCACATACACAGGATTTTGC	AGCTGCAGCGCCCTCT
Danio rerio	*csf3r*	CCTCCGGTGTGACTGGAATC	ACCTTTTGTGACTTGGCCCTAA
Danio rerio	*mpx*	GAGGTTCCTTGCTTCATTG	GCACATGAAGGGCGCGAGCC
Danio rerio	*lyz*	GCAGGTTTAAGACCCACCGA	TTCAGCCCGTCCATTTTCAC
Mus musculus	*Gapdh*	AGGTCGGTGTGAACGGATTTG	TGTAGACCATGTAGTTGAGGTCA
Mus musculus	*Phf8*	AGGTTCCTGTCAGTGTGTGT	TCTCTAGACGATGGCTGACA
Mus musculus	*C/ebp α*	GCAAAGCCAAGAAGTCGGTG	TCTCCACGTTGCGTTGTTTG
Mus musculus	*Znf711*	CTTGAAGCCGATGTTGCCATT	TCAGCCACAAAAACCTGCTCA
Homo sapiens	*GAPDH*	ACAACTTTGGTATCGTGGAAGG	GCCATCACGCCACAGTTTC
Homo sapiens	*GFI1*	CCGCGCTCATTTCTCGTCA	ACGGAGGGAATAGTCTGGTCC
Homo sapiens	*ZNF711*	ATGGATTCAGGCGGTGGAAG	CAGCCATTCCAGCCACAAAA
Homo sapiens	*PHF8*	GCTTCTCGAAGCCCCTG	TGGACGATAGCGCGGC

Primers for ChIP-qPCR

Species	**Gene**	**Forward (5'-3')**	**Reverse (5'-3')**
Danio rerio	*c/ebpα*-NP	AGGAAAGCATTAGGACCGCC	GCCACACGGGATCTCCTTTA
Danio rerio	*c/ebpα*-PP	GTCCGCGCTTACCTCTTCTC	GGTGCAAGTGGGAAATGTGC
Danio rerio	*znf711*-NP	CTCCCAAGGTTGTGAATCGGT	GTCACTCTCAGCGTCCCAAT
Danio rerio	*znf711*-PP	CGGAGTAGTGGACAAGCTGTT	CCTGTAAAGATCGGCCCACA

Primers for plasmid construction

Species	Plasmid	Forward (5'-3')	Reverse (5'-3')
Danio rerio	HA-*znf711*	CCATCGATATGTACCCATACGATGTTCCAGATTACGCTATGGATCAAGGTGGAGGGATCCTG	CCCTCGAGTTATAACAGGGTTTCCTTGTGATG
Danio rerio	HA-*znf711*-Δ DBD	GTTCCAGATTACGCTGAATTCATGGATCAAGGTGGAGGGATCC	ACGACTCACTATAGTTCTAGATTACAGTGGCTGCCCATCAGG
Danio rerio	HA-*znf711*-Δ Zfx/y	GTTCCAGATTACGCTGAATTCACTGTATACCCCTGTCACATCTGTGG	ACGACTCACTATAGTTCTAGATTATAACAGGGTTTCCTTGTGATGTC
Danio rerio	HA-*gfi1aa*	GTTCCAGATTACGCTGAATTCATGCCGAGGTCATTTTTGGTG	ACGACTCACTATAGTTCTAGATTATTTTAGCCCGTGCTGTGTTT
Danio rerio	Flag-*phf8*	GACGATGACGACAAGGAATTCATGGCATCTGTTCCGGTTTACT	ACGACTCACTATAGTTCTAGACTACAGCAGCAGCTTGCCG
Danio rerio	Flag-*phf8*-Δ PhD	GCATCTGTTCCGGGACCATCTGTC	GACAGATGGTCCCGGAACAGATGC
Danio rerio	Flag-*phf8*-Δ JmjC	TTCTCAGACACCGAAAAGATCTTT	AAAGATCTTTTCGGTGTCTGAGAA
Danio rerio	TOL2(*mpx:c/ebpα*)	AATATGTGTTTTTAGGGATCCATGGAGCAAGCAAACCTCTACG	CCTCGCCCTTGCTCACCATGGTTAAGCGCAGTTGCCCATG
Danio rerio	Tol2(*mpx:c/ebpα*-bZIP)	AATATGTGTTTTTAGGGATCCAAGAACAGCACCGAGTACAGGC	CCTCGCCCTTGCTCACCATGGGCCCCGTAACGTCTCCAGTT

Danio rerio	Tol2(*mpx*:*PHF8*)	AATATGTGTTTTTAGGGATCCATGGCCTCGGTGCCGGTG	CCTCGCCCTTGCTCACCATGGTCACAGAAGTAGTTTGCCATTTCTG
Danio rerio	Tol2(*mpx*:*PHF8*^{K840R})	CCTCCTGAGCCTAGACAAGAGGCCCTG	CAGGGCCTCTTGTCTAGGCTCAGGAGG
Danio rerio	Tol2(*mpx*:*PHF8*^{K840R}-*SUMO1*)	GCAAACTACTTCTGACCATGGATGTCAGACACGGAGACCAAGC	CCTCGCCCTTGCTCACCATGGCTAGTCGTTCCGACAGCCTCC
Danio rerio	HA-*sumo1*	GTTCCAGATTACGCTGAATTCATGTCAGACACGGAGACCAAGC	ACGACTCACTATAGTTCTAGACTAGTCGTTCCGACAGCCTCC
Homo sapiens	HA-*ZNF711*-S	CGGGATCCATGTACCCATACGATGTTCCAGATTACGCTATGGATTCAGGCGGTGGAAGTCTT	CCCTCGAGTTACATAAGAGCCTCTTTGTGGTG
Homo sapiens	HA-*ZNF711*-L	GATATCAGTTGCGCTGAAATAGCAGATGAAGTTTACATGGAAGTCATTGTAGGGGAAGAGGAAGGAACTTCTCTCCCTGAGATTCAGCTTGAGGACTCTGATGTTAATAAAACAGTTGTCCCTGTTGTCTGGGCTGCGGCATATGGAGATGAAAGAAGAGTTTCCCG	ATCTTCTTCTTGAGAAGAAT
Homo sapiens	FLAG-*PHF8*	GACGATGACGACAAGGAATTCATGGCCTCGGTGCCGGTG	ACGACTCACTATAGTTCTAGATCACAGAAGTAGTTTGCCATTTCTG

Homo sapiens	FLAG-*PHF8*^{K840R}	CCTCCTGAGCCTAGA CAAGAGGCCCTG	CAGGGCCTCTTGTCTAGGC TCAGGAGG

Primers for PLVX-shRNA generation

Species	**Gene**	**Forward (5'-3')**	**Reverse (5'-3')**
Homo sapiens	*ZNF711*	GATCCGCCAATGTGAGTATT GTGAATATTCAAGAGATATTC ACAATACTCACATTGGTTTTT TG	AATTCAAAAAACCAATGTGAGT ATTGTGAATATCTCTTGAATATT CACAATACTCACATTGG CG
Homo sapiens	*PHF8*	GATCCGCTGGCCAGTTGAGC TATAATTTCAAGAGAATTATA GCTCAACTGGCCAGCTTTTT TG	AATTCAAAAAAGCTGGCCAGTT GAGCTATAATTCTCTTGAAATTA TAGCTCAACTGGCCAGC G

Primers for pLKO.1-shRNA generation

Homo sapiens	*GFI1*	CCGGCATCAAGTGCAGCAA GGTGTTCTCGAGAACACCTT GCTGCACTTGATGTTTTTT	AATTAAAAAACATCAAGTGCAG CAAGGTGTTCTCGAGAACACCT TGCTGCACTTGATG

Primers for luciferase assays

Species	**Gene**	**Forward (5'-3')**	**Reverse (5'-3')**
Danio rerio	*c/ebpα* promoter (-0.6~-0.9k)	GGGGTACCCCAA TGTTTATTTGTGT GTGAATAAAT	CCCTCGAGGGTGTTTCTTAAC GTTTTGATGCTCA
Danio rerio	*znf711* promoter (-2.0k)	GCGTGCTAGCCC GGGCTCGAGTTT TAATCGTATTCAA AAACTTGTTTGA	ACTTAGATCGCAGATCTCGAG TCCGTTTCAGCCAACCAGAC

Primers for CRISPR/Cas9 genotyping

Species	Gene	Forward (5'-3')	Reverse (5'-3')
Danio rerio	*znf711*	CTCTCAGAACAAAGGCCTGA	TGTCACCACATCTGACACCA
Danio rerio	*phf8*	CGAGTTTCTTCGCAGGTGTT	GTCTGCTTGGCGACTGACAT
Danio rerio	*gfi1aa*	CCGGACAGGCTCCTGAAAGCC	TGAGCGGTCACACACACTGCC

Supplemental Methods

Zebrafish maintenance and mutant generation

Zebrafish were raised, bred, and staged according to standard protocols [1]. The following strains were used: AB, *Tg(mpx:eGFP)rj30* (ZFIN database). For CRISPR9 mediated *znf711* and *phf8* knockout zebrafish generation, guide RNAs (gRNA) targeting the exon 4 of *znf711*, and the exon 5 of *phf8*, were designed using an online tool ZiFiT Targeter software (http://zifit.partners.org/ZiFiT), which were synthesized by cloning the annealed oligonucleotides into the gRNA transcription vector. Cas9 mRNA and gRNA were co-injected into one-cell stage zebrafish embryos. The injected F0 founder embryos were raised to adulthood and then outcrossed with wild-type zebrafish. F1 embryos carrying potential indel mutations were raised to adulthood. Then PCR amplification and sequencing were performed on genomic DNA isolated from tail clips of F1 zebrafish to identify mutants. Both *znf711* and *phf8* lines produce truncated proteins that lack functional domains.

Whole-mount *in situ* hybridization (WISH)

Digoxigenin-labeled RNA probes were transcribed with T7, T3 or SP6 polymerase (Ambion, Life Technologies, Carlsbad, USA). WISH was performed as described previously [2]. The probes labeled by digoxigenin were detected using alkaline phosphatase coupled anti-digoxigenin Fab fragment antibody (Roche, Basel, Switzerland) with 5-bromo-4-chloro-3-indolyl-phosphate nitro blue tetrazolium staining (Vector Laboratories, Burlingame, CA, USA). At least 15 ~ 30 embryos or

larvae were used for each probe. The positive signals were counted under a microscope, and the mean value was obtained from the counts of all of the embryos/larvae in the same group.

Sudan Black staining

The zebrafish larvae treated with 4% paraformaldehyde (PFA) overnight at 4˚C were incubated with a Sudan Black (Sigma-Aldrich, St. Louis, MO, USA) solution for about 30 minutes to detect the granules of granulocytes. The detailed method was described previously [3]. Staining was then observed under a microscope.

FACS analysis and Cell collection

FACS analysis and cell collection were performed as previously described [4]. Wild-type *Tg(mpx:eGFP)* and *znf711*$^{-/-}$//*Tg(mpx:eGFP)* larvae were dissociated into single cells using 0.05% trypsin (Sigma-Aldrich, St. Louis, MO, USA) as previously described [5]. These dissociated cells were passed through a 40-μm mesh, centrifuged at 450g, and suspended in 5% FBS/PBS before addition of propidium iodide to a final concentration of 1 μg/ml for exclusion of dead cells. wild-type zebrafish (without GFP) were used as blank to determine the background values in GFP-controls. The GFP^{+} cells of each group were collected from a total of ~ 1000 larvae using a FACS Vantage flow cytometer (Beckton Dickenson) (~ 300 larvae once, performed 3 times). For the whole kidney marrow (WKM) samples, FACS analysis was based on forward and side scatter characteristics, propidium iodide exclusion and GFP fluorescence. The GFP^{+} cells in the myeloid gate was enriched from WKM samples of wild-type *Tg(mpx:eGFP)* and *znf711*$^{-/-}$//*Tg(mpx:eGFP)* zebrafish (one-year-old, each time one male and one female were used in the WT and mutant groups, respectively).

RNA sequencing and Quantitative RT-PCR

At 48 hpf, GFP positive cells were isolated from either wild-type *Tg(mpx:eGFP)* or *znf711* MO injected *Tg(mpx:eGFP)* larvae by FACS. mRNA was extracted from

sorted cells using RNeasy Micro (Qiagen, Manchester, UK) and mRNA libraries were constructed using the VAHTS Universal V8 RNA-seq Library Prep Kit (vazyme Technology Co., Ltd., Nanjing, China). Then libraries with different indexs were multiplexed and loaded on a Navoseq6000 instrument for sequencing using a 2 x 150 paired-end (PE) configuration according to manufacturer's instructions.

The quantitative PCR was carried out with SYBR Green Real-time PCR Master Mix (TOYOBO, Osaka, Japan) with ABI 7900HT real-time PCR machine and analyzed with Prism software. *β-actin* was served as the internal control. The primers used are listed in Table S1. Each time a different batch of samples was used. The expression levels of each interested gene were normalized to internal control *β-actin* by real-time qPCR and compared with WT group which was set to 1.0. Real time qPCR was performed with gene specific primers and gene expression levels were analyzed by comparative CT method.

Plasmid construction

Zebrafish *znf711* and its serial mutants were cloned into pCS2^{+} vector. For the luciferase reporter, the promoter (-600 bp ~ -960 bp) of zebrafish *c/ebpα* was cloned into the PGL3 basic vector (Promega, Madison, WI, USA). Primers used were listed in Table S1.

Morpholino and mRNA synthesis for microinjection

Morpholinos for *znf711* (5'-AGATTATGGATCAAGGTGGAGGGAT-3'), *phf8* (5'-ATGGCATCTGTTCCGGTTTACTGCC-3'), and *gfi1aa* (5'-GTAAACATGCCGAGGTCATTTTTGG-3') were designed and purchased from Gene Tools. Full-length capped mRNA samples were all synthesized from linearized plasmids using the mMessage mMachine SP6 kit (Invitrogen, Thermo Fisher, Waltham, USA). Microinjection concentration of mRNA was between 50 ~ 200 ng/μl and 2 nl of mRNA was injected at one-cell stage embryos. All injections were performed with a Harvard Apparatus micro-injector.

Cell culture and dual-luciferase reporter assay

HEK293T cells were maintained in DMEM (Gibco, Life technologies, Carlsbad, USA) with 10% Fetal Bovine Serum (Gibco, Life technologies, Carlsbad, USA). Plasmid transfection was carried out with Effectene Transfection Reagent (Qiagen, Manchester, UK) according to manufacturer's instruction. For the luciferase reporter assay, cells were harvested 48 hours after transfection and analyzed using the Dual Luciferase Reporter Assay Kit (Beyotime, Shanghai, China), according to the manufacturer's protocols.

Co-immunoprecipitation and western blot assay

HEK293T cells, which had been transfected with plasmids for 48 hours, were washed with phosphate-buffered saline (PBS) buffer for 1 minute 3 times. Lysates were prepared using RIPA lysis buffer (Beyotime, Shanghai, China) with proteinase inhibitor (Roche, Basel, Switzerland), after shaking on ice for 30 minutes, the cells were harvested and centrifuged at 15,000 × g for 30 min. Antibody indicated in the results (Cell Signaling Technology) was mixed with the protein-G-agarose beads (30 μl) in the supernatant at 4˚C overnight. The beads were prepared by centrifugation and washed three times with RIPA lysis buffer. Proteins binding to the beads were eluted by adding 30 μl of 2× SDS sample buffer and analyzed by immunoblotting using antibody indicated (Cell Signaling Technology).

Chromatin immunoprecipitation qPCR (ChIP-qPCR)

For ChIP analysis, GFP and GFP-Znf711 expressing larvae were harvested at 48 hpf for brief fixation. Cross-linked chromatin was immunoprecipitated with anti-GFP antibody according to the procedure described (Cell Signaling Technology) [6]. The resultant immunoprecipitated samples were subjected to quantitative PCR using primer pairs (Table S1).

The genomic regions targeted by ChIP-qPCR were selected as follows: putative

binding sites for sequence-specific transcription factor C/EBPα were predicted at JASPAR website; regions for the chromatin-associated co-regulator PHF8, which lacks a defined DNA-binding motif, were chosen based on its occupancy peaks in public ChIP-seq datasets (Cistrome Database).

Cell line and treatment

32Dcl3 cells were maintained in 1640 (Life technologies, Grand Island, NY, USA) with 10% Fetal Bovine Serum (Life technologies, Grand Island, NY, USA) and 1 ng/ml murine IL-3 (PeproTech, USA). 32Dcl3 cells were treated with 1 μM of ATRA (Sigma Aldrich, St. Louis, MO, USA) for 72 hours.

KEY RESOURCES TABLE

REAGENT or RESOURCE	**SOURCE**	**IDENTIFIER**
Antibodies		
ZNF711 Polyclonal Antibody	Abcam	Cat#AB254776
GFI1 Polyclonal Antibody	Santa Cruz Biotechnology	Cat#sc-373960
PHF8 Polyclonal Antibody	Bethyl Laboratories	Cat# A301-772A
Normal Rabbit IgG	Cell Signaling Technology	Cat#2729P
Anti-HA tag ChIP-Grade	Abcam	Cat#ab9110
Rabbit monoclonal anti-HA	Cell Signaling Technology	Cat#3724
Rabbit monoclonal anti-FLAG	Cell Signaling Technology	Cat#14793
Mouse monoclonal anti-GAPDH	Proteintech	Cat#60004-1-Ig
Chemicals, peptides, and recombinant proteins		
ATRA	Sigma-Aldrich	Cat#R2625
Recombinant Murine IL-3	PeproTech	Cat#213-13
Critical Commercial Assays		
SimpleChIP® Plus Sonication Chromatin IP Kit	Cell Signaling Technology	Cat#56383S

Dual-Lumi™ Luciferase Reporter Gene Assay Kit	Beyotime	Cat#RG088S
Experimental Models: Cell Lines		
Human: HEK293T	ATCC	CRL-11268
Mouse: 32D Clone3	ATCC	CRL-3594
Software and algorithms		
ImageJ	NIH	N/A
GraphPad Prism 9.0	Graphpad, Inc	N/A

References

1. Kimmel CB, Ballard WW, Kimmel SR, Ullmann B, Schilling TF. Stages of embryonic development of the zebrafish. Dev Dyn 1995;203(3):253–310.

2. Thisse C, Thisse B. High-resolution in situ hybridization to whole-mount zebrafish embryos. Nat Protoc 2008;3(1):59–69.

3. Le Guyader D, Redd MJ, Colucci-Guyon E, et al. Origins and unconventional behavior of neutrophils in developing zebrafish. Blood 2008;111(1):132–141.

4. Traver D, Paw BH, Poss KD, Penberthy WT, Lin S, Zon LI. Transplantation and in vivo imaging of multilineage engraftment in zebrafish bloodless mutants. Nat Immunol 2003;4(12):1238–1246.

5. Yan C, Huo X, Wang S, Feng Y, Gong Z. Stimulation of hepatocarcinogenesis by neutrophils upon induction of oncogenic kras expression in transgenic zebrafish. J Hepatol 2015;63(2):420–428.

6. Hart DO, Raha T, Lawson ND, Green MR. Initiation of zebrafish haematopoiesis by the TATA-box-binding protein-related factor Trf3. Nature 2007;450(7172):1082–1085.